Available online at www.sciencedirect.com
SCIENCE DIRECT®
Journal of Computational Physics 211 (2006) 9–35
JOURNAL OF COMPUTATIONAL PHYSICS
www.elsevier.com/locate/jcp

Conservative space-time mesh refinement methods for the FDTD solution of Maxwell's equations

F. Collino [a], T. Fouquet [b], P. Joly [c,*]

[a] CERFACS, Toulouse, France
[b] E.D.F. Clamart, France
[c] INRIA, Rocquencourt, Domaine de Voluceau, BP105, F-78153 Le Chesnay, Cedex, France

Received 18 October 2004; received in revised form 1 March 2005; accepted 9 March 2005
Available online 15 August 2005

Abstract

A new variational space-time mesh refinement method is proposed for the FDTD solution of Maxwell's equations. The main advantage of this method is to guarantee the conservation of a discrete energy that implies that the scheme remains L^2 stable under the usual CFL condition. The only additional cost induced by the mesh refinement is the inversion, at each time step, of a sparse symmetric positive definite linear system restricted to the unknowns located on the interface between coarse and fine grid. The method is presented in a rather general way and its stability is analyzed. An implementation is proposed for the Yee scheme. In this case, various numerical results in 3-D are presented in order to validate the approach and illustrate the practical interest of space-time mesh refinement methods.

1. Introduction

Although very old, finite difference time domain methods (FDTD in the electro-magnetic literature) remain very popular and are widely used in wave propagation simulations or more generally for the solution of linear hyperbolic systems among which Maxwell's system is a typical example. These methods allow us to get discrete equations whose unknowns are generally field values at the points of a regular mesh with spatial step h and time step Δt. The numerical schemes that interest us are explicit: applying an explicit formula provides the solution at time $t + \Delta t$ from the solution at, or before, time t. For Maxwell's equations, the Yee scheme [15,23] is a prototype of such a scheme. This scheme is centered, of order two both in space and time, and completely explicit. There are several reasons for the success of Yee type schemes, among

* Corresponding author. Tel.: +33 01 3963 5448.
E-mail address: patrick.joly@inria.fr (P. Joly).

0021-9991/$ - see front matter © 2005 Published by Elsevier Inc.
doi:10.1016/j.jcp.2005.03.035

which their easy implementation and the fact that a lot of properties of continuous Maxwell's equations (discrete energy conservation, free divergence property, etc.) are respected at the discrete level. The stability and accuracy properties of this scheme are well known. A negative consequence of its explicit nature is that the scheme is stable only under some stability CFL condition, which, in a homogeneous medium, can be written as

$$\frac{c\Delta t}{h} \leqslant \frac{\sqrt{d}}{d},$$

where c denotes the propagation velocity of the waves and d the space dimension. This imposes that the time step cannot be too large. This is not restrictive in practice since a sufficient accuracy requires a small time step. On the other hand, Δt must not be too small either because, as is well known, the numerical dispersion, roughly speaking the error committed on the propagation velocity of waves, increases when the ratio $c\Delta t/h$ decreases [8].

Of course, one of the drawbacks of such a method is a lack of "geometrical flexibility". In order to treat complex geometries or geometrical details in diffraction problems, a natural idea is to use local mesh refinements. Moreover, with finite difference methods, it is necessary to be able to treat non-matching grids (see Fig. 1).

A first possibility consists in using only spatial refinement (see [1] for acoustic waves, [3] and [20] for Maxwell's equations). However, when a uniform time step is used, it is the finest mesh that will dictate the time step because of the stability condition. Therefore, the computational costs will increase and, moreover, the ratio $c\Delta t/h$ being much smaller than its optimal value in the coarse grid, one will generate dispersion errors. A way to avoid these problems is to use a local time step Δt, related to h in order to keep the ratio $c\Delta t/h$ constant everywhere in the computational domain. This is why the question we addressed at the beginning of this work was the following: how to do space-time mesh refinement with Yee's scheme in such a way that the stability of the coupling scheme is theoretically guaranteed and the stability condition is not affected by the mesh refinement? This question appears much more delicate than in the case of a simple spatial refinement. The numerous solutions suggested in the electro-magnetic literature are primarily based on interpolation techniques (in time and/or in space) especially designed to guarantee the consistency of the

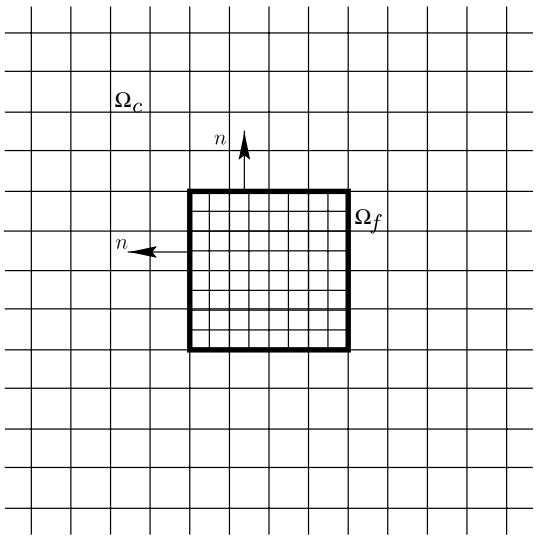

Fig. 1. 2-D slice of the domains Ω_f and Ω_c. Domain Ω_c is infinite and surrounds Ω_f.

scheme at the coarse grid–fine grid interface (see for instance [19,18,22,7]). Unfortunately, the resulting schemes appear to be very difficult to analyze and may suffer from some instability problems as shown in [9] (see Fig. 2).

This is why we have developed an alternative approach that we shall present here in the case of two spatial grids: one is twice as fine than the other (however the method extends to stronger refinement). This method appears as an extension to higher dimensions of the method introduced in [10–12] for the 1-D wave equation. It is based on three major features, namely, the reinterpretation of Yee's scheme as a particular mixed finite element scheme, a domain decomposition approach with the introduction of a Lagrange multiplier at the interface (as for the mortar element method), and finally – this is the most original point – a specific time discretization procedure of the variational interface conditions that guarantees a priori the stability of the scheme via the conservation of an appropriate discrete energy (see Fig. 3).

In our presentation, we shall show a general abstract framework to which our strategy can be applied. That is why our method is not limited to Maxwell's equations and Yee's scheme. It can also be applied to a large class of problems including acoustics, elastodynamics, fluid–structure interaction, etc., and can be generalized for instance to general finite elements (which can be of a different order in each domain).

The outline of our article is as follows. In Section 1, we formulate the problem as a transmission problem and derive the variational formulation that will be the basis of the discretization procedure. We describe this procedure in Section 2. We present the abstract space discretization in Section 2.1 and the time discretization in Section 2.2 (which is the central section of the paper). We address in particular the questions of the existence of the discrete solution and of the stability of the method. In Section 3, we apply our general procedure to the specific case of the Yee's scheme. Section 4 is devoted to the presentation of various numerical results, which in particular emphasize the interest of applying local mesh refinement.

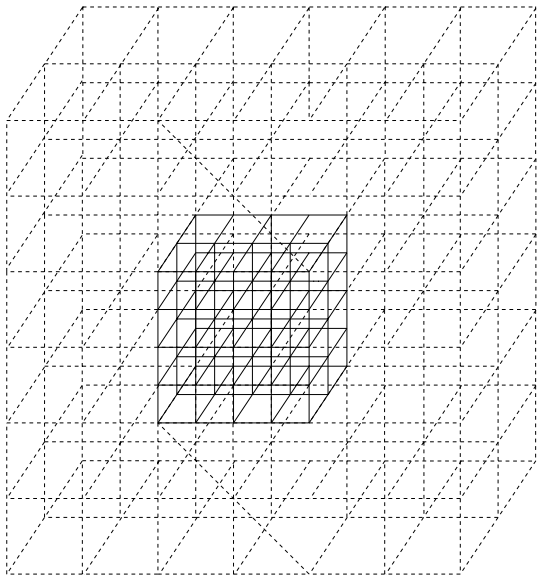

Fig. 2. 3-D view of the refinement.

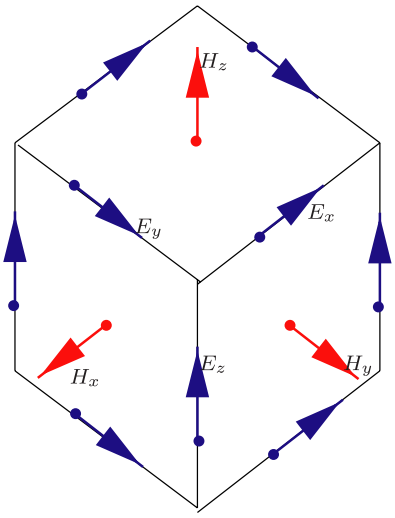

Fig. 3. Degrees of freedom of E and H.

2. Presentation of the method

2.1. The model problem

As a model problem, we consider (E,H), a solution of the Maxwell's system in the whole space:

$$\begin{aligned} &\epsilon_0 \partial_t E(x,t) - \mathrm{curl} H(x,t) = 0, \quad x \in \mathbf{R}^3, \\ &\mu_0 \partial_t H(x,t) + \mathrm{curl} E(x,t) = 0, \quad x \in \mathbf{R}^3. \end{aligned} \tag{1}$$

Initial conditions are given at $t = 0$. Source terms could also be added but are omitted to simplify the presentation. Our goal is to solve numerically this problem by domain decomposition using locally a grid which is twice as fine as the grid in the rest of the domain. To be more specific, we consider a parallelepipedic box Ω_f with boundary Σ. We denote by $n(x)$ the outward (with respect to Ω_f) unit normal vector on Σ at point x. The domain Ω_f is the one that we shall discretize with a fine grid of step h and Ω_c is the one that we shall discretize with a coarse grid of step $2h$. In what follows, (E_c,H_c) will denote the restriction to Ω_c of the electro-magnetic field (index c refers to the "coarse grid domain") while (E_f,H_f) will denote the restriction to Ω_f of the electro-magnetic field (index f refers to the "fine grid domain").

2.2. A 2-domain formulation

The fields E_c, H_c and E_f, H_f are solutions of Maxwell's equations in Ω_c and Ω_f, respectively, and are coupled through the continuity of the tangential traces of the electro-magnetic fields across Σ. This allows us to reformulate the problem as follows. We introduce as an additional unknown the common "tangential trace" of the magnetic fields H_c and H_f on the interface, more precisely,

$$J(x,t) = (H_c)_{|\Sigma}(x,t) \wedge n(x) = (H_f)_{|\Sigma}(x,t) \wedge n(x). \tag{2}$$

Note that J is the electric current flowing on the surface Σ. If we assume that J is known, (E_c,H_c) and (E_f,H_f) are the respective solutions of the two following uncoupled boundary value problems, in which J appears as a source term:

$$\begin{cases} \epsilon_0 \partial_t E_{\mathrm{f}}(x,t) - \mathrm{curl} H_{\mathrm{f}}(x,t) = 0, \quad x \in \Omega_{\mathrm{f}}, & \text{(i)} \\ \mu_0 \partial_t H_{\mathrm{f}}(x,t) + \mathrm{curl} E_{\mathrm{f}}(x,t) = 0, \quad x \in \Omega_{\mathrm{f}}, & \text{(ii)} \\ H_{\mathrm{f}}(x,t) \wedge n(x) = J(x,t), \quad x \in \Sigma = \partial\Omega_{\mathrm{f}}, \end{cases} \tag{3}$$

$$\begin{cases} \epsilon_0 \partial_t E_{\mathrm{c}}(x,t) - \mathrm{curl} H_{\mathrm{c}}(x,t) = 0, \quad x \in \Omega_{\mathrm{c}}, & \text{(i)} \\ \mu_0 \partial_t H_{\mathrm{c}}(x,t) + \mathrm{curl} E_{\mathrm{c}}(x,t) = 0, \quad x \in \Omega_{\mathrm{c}}, & \text{(ii)} \\ H_{\mathrm{c}}(x,t) \wedge n(x) = J(x,t), \quad x \in \Sigma = \partial\Omega_{\mathrm{c}}. \end{cases} \tag{4}$$

By construction, there is continuity of the tangential component of the magnetic field across the interface between the two domains. The idea of the method is to consider J as a control variable in order to ensure the continuity of the tangential electric field

$$n(x) \wedge \big(E_{\mathrm{f}|\Sigma}(x,t) \wedge n(x)\big) = n(x) \wedge \big(E_{\mathrm{c}|\Sigma}(x,t) \wedge n(x)\big). \tag{5}$$

Our method of approximation will rely on the formulation (3)–(5).

Remark 1. The proof of the equivalence between problem (1) and (3)–(5) would be classical and easy if the boundary Σ were smooth. In the case of a non-smooth Σ, a rigorous proof relies on trace theorems in the space $H(\mathrm{curl},\Omega_{\mathrm{f}})$ for polyhedral domain Ω_{f} and related Green's formula (see [6]).

The next step consists of establishing a mixed variational formulation of the coupled problem (3)–(5).

2.3. An abstract variational formulation

The functional framework is the following. We look for the electro-magnetic fields:

$$\begin{aligned} E_{\mathrm{f}}(t) :\ & \mathbf{R}^+ \ \rightarrow \ V_{\mathrm{f}} = H(\mathrm{curl}, \Omega_{\mathrm{f}}), \\ H_{\mathrm{f}}(t) :\ & \mathbf{R}^+ \ \rightarrow \ W_{\mathrm{f}} = L^2(\Omega_{\mathrm{f}}), \\ E_{\mathrm{c}}(t) :\ & \mathbf{R}^+ \ \rightarrow \ V_{\mathrm{c}} = H(\mathrm{curl}, \Omega_{\mathrm{c}}), \\ H_{\mathrm{c}}(t) :\ & \mathbf{R}^+ \ \rightarrow \ W_{\mathrm{c}} = L^2(\Omega_{\mathrm{c}}), \\ J(t) :\ & \mathbf{R}^+ \ \rightarrow \ M = \mathbf{H}_{\|}^{-1/2}(\mathrm{div}_\Sigma, \Sigma), \end{aligned} \tag{6}$$

where the space $\mathbf{H}_{\|}^{-1/2}(\mathrm{div}_\Sigma, \Sigma)$ is precisely defined in [6]. This space is the image of V_{f} or V_{c} by the trace map

$$\gamma_\tau u = u \wedge n_{|\Sigma}.$$

We shall denote by π_τ the trace map

$$\pi_\tau u = n \wedge (u \wedge n)_{|\Sigma},$$

which maps the spaces V_{f} and V_{c} continuously onto the dual space of M, $M' = \mathbf{H}_{\perp}^{-1/2}(\mathrm{curl}_\Sigma, \Sigma)$ [6]. Finally, we shall denote by $\langle\cdot,\cdot\rangle$ the duality product between M and M', which is the natural extension of the inner product in $L^2(\Sigma)^3$.

Using the following Green's formulae:

$$\begin{cases} \int_{\Omega_{\mathrm{f}}} (\mathrm{curl} v \cdot u - \mathrm{curl} u \cdot v)\, \mathrm{d}x = \langle \gamma_\tau u, \pi_\tau v \rangle \quad \forall u, v \in \mathbf{H}(\mathrm{curl}, \Omega_{\mathrm{f}}), \\ \int_{\Omega_{\mathrm{c}}} (\mathrm{curl} v \cdot u - \mathrm{curl} u \cdot v)\, \mathrm{d}x = -\langle \gamma_\tau u, \pi_\tau v \rangle \quad \forall u, v \in \mathbf{H}(\mathrm{curl}, \Omega_{\mathrm{c}}), \end{cases} \tag{7}$$

it is easy to establish the following weak formulation of problem (3)–(5): Eqs. (i) and (ii) of (3) and (4) are multiplied by appropriate test fields then integrated in space. We integrate by parts the terms involving the curl of the magnetic field:

$$\begin{cases} \frac{\mathrm{d}}{\mathrm{d}t}\int_{\Omega_\mathrm{f}} \epsilon_0 E_\mathrm{f}(x,t)\cdot\tilde{E}_\mathrm{f}(x)\,\mathrm{d}x - \int_{\Omega_\mathrm{f}} \mathrm{curl}\tilde{E}_\mathrm{f}(x)\cdot H_\mathrm{f}(x,t)\,\mathrm{d}x = -\langle J(.,t), \pi_\tau \tilde{E}_\mathrm{f}\rangle & \forall \tilde{E}_\mathrm{f}\in V_\mathrm{f}, \\ \frac{\mathrm{d}}{\mathrm{d}t}\int_{\Omega_\mathrm{f}} \mu_0 H_\mathrm{f}(x,t)\cdot\tilde{H}_\mathrm{f}(x)\,\mathrm{d}x + \int_{\Omega_\mathrm{f}} \mathrm{curl}E_\mathrm{f}(x,t)\cdot\tilde{H}_\mathrm{f}(x)\,\mathrm{d}x = 0 & \forall \tilde{H}_\mathrm{f}\in W_\mathrm{f}, \end{cases} \tag{8}$$

$$\begin{cases} \frac{\mathrm{d}}{\mathrm{d}t}\int_{\Omega_\mathrm{c}} \epsilon_0 E_\mathrm{c}(x,t)\cdot\tilde{E}_\mathrm{c}(x)\,\mathrm{d}x - \int_{\Omega_\mathrm{c}} \mathrm{curl}\tilde{E}_\mathrm{c}(x)\cdot H_\mathrm{c}(x,t)\,\mathrm{d}x = \langle J(.,t), \pi_\tau \tilde{E}_\mathrm{c}\rangle & \forall \tilde{E}_\mathrm{c}\in V_\mathrm{c}, \\ \frac{\mathrm{d}}{\mathrm{d}t}\int_{\Omega_\mathrm{c}} \mu_0 H_\mathrm{c}(x,t)\cdot\tilde{H}_\mathrm{c}(x)\,\mathrm{d}x + \int_{\Omega_\mathrm{c}} \mathrm{curl}E_\mathrm{c}(x,t)\cdot\tilde{H}_\mathrm{c}(x)\,\mathrm{d}x = 0 & \forall \tilde{H}_\mathrm{c}\in W_\mathrm{c}, \end{cases} \tag{9}$$

$$\langle J', \pi_\tau E_\mathrm{f}(.,t)\rangle = \langle J', \pi_\tau E_\mathrm{c}(.,t)\rangle \quad \forall J'\in M. \tag{10}$$

This problem enters into the framework of general abstract evolution problems of mixed type: Find $(E_\mathrm{c}(t),H_\mathrm{c}(t),E_\mathrm{f}(t),H_\mathrm{f}(t),J(t)) : \mathbf{R}^+ \to V_\mathrm{c}\times W_\mathrm{c}\times V_\mathrm{f}\times W_\mathrm{f}\times M$ such that:

$$\begin{cases} \frac{\mathrm{d}}{\mathrm{d}t}\epsilon_\mathrm{c}(E_\mathrm{c},\tilde{E}_\mathrm{c}) - b_\mathrm{c}(\tilde{E}_\mathrm{c},H_\mathrm{c}) + c_\mathrm{c}(J,\tilde{E}_\mathrm{c}) = 0 & \forall \tilde{E}_\mathrm{c}\in V_\mathrm{c}, \\ \frac{\mathrm{d}}{\mathrm{d}t}\mu_\mathrm{c}(H_\mathrm{c},\tilde{H}_\mathrm{c}) + b_\mathrm{c}(E_\mathrm{c},\tilde{H}_\mathrm{c}) = 0 & \forall \tilde{H}_\mathrm{c}\in W_\mathrm{c}, \end{cases} \tag{11}$$

$$\begin{cases} \frac{\mathrm{d}}{\mathrm{d}t}\epsilon_\mathrm{f}(E_\mathrm{f},\tilde{E}_\mathrm{f}) - b_\mathrm{f}(\tilde{E}_\mathrm{f},H_\mathrm{f}) - c_\mathrm{f}(J,\tilde{E}_\mathrm{f}) = 0 & \forall \tilde{E}_\mathrm{f}\in V_\mathrm{f}, \\ \frac{\mathrm{d}}{\mathrm{d}t}\mu_\mathrm{f}(H_\mathrm{f},\tilde{H}_\mathrm{f}) + b_\mathrm{f}(E_\mathrm{f},\tilde{H}_\mathrm{f}) = 0 & \forall \tilde{H}_\mathrm{f}\in W_\mathrm{f}, \end{cases} \tag{12}$$

$$c_\mathrm{c}(\tilde{J},E_\mathrm{c}) = c_\mathrm{f}(\tilde{J},E_\mathrm{f}) \qquad \forall \tilde{J}\in M, \tag{13}$$

where:

- U_c, W_c, U_f and W_f are Hilbert spaces,
- ϵ_c (respectively, ϵ_f) is a continuous bilinear form on $V_\mathrm{c}\times V_\mathrm{c}$ (respectively, $V_\mathrm{f}\times V_\mathrm{f}$),
- μ_c (respectively, μ_f) is a continuous bilinear form on $W_\mathrm{c}\times W_\mathrm{c}$ (respectively, $W_\mathrm{f}\times W_\mathrm{f}$),
- b_c (respectively, b_f) is a continuous bilinear form on $V_\mathrm{c}\times W_\mathrm{c}$ (respectively, $V_\mathrm{f}\times W_\mathrm{f}$),
- c_c (respectively, c_f) is a continuous bilinear form on $M\times V_\mathrm{c}$ (respectively, $M\times V_\mathrm{f}$).

In our case, we have:

$$\begin{aligned} &\epsilon_\mathrm{c}(\tilde{E},\tilde{E}) = \int_{\Omega_\mathrm{c}} \epsilon_0\tilde{E}\cdot\tilde{E}\,\mathrm{d}x, \quad \epsilon_\mathrm{f}(\tilde{E},\tilde{E}) = \int_{\Omega_\mathrm{f}} \epsilon_0\tilde{E}\cdot\tilde{E}\,\mathrm{d}x, \\ &\mu_\mathrm{c}(\tilde{H},\tilde{H}) = \int_{\Omega_\mathrm{c}} \mu_0\tilde{H}\cdot\tilde{H}\,\mathrm{d}x, \quad \mu_\mathrm{f}(\tilde{H},\tilde{H}) = \int_{\Omega_\mathrm{f}} \mu_0\tilde{H}\cdot\tilde{H}\,\mathrm{d}x, \\ &b_\mathrm{c}(\tilde{E},\tilde{H}) = \int_{\Omega_\mathrm{c}} \tilde{H}\cdot\mathrm{curl}\tilde{E}\,\mathrm{d}x, \quad b_\mathrm{f}(\tilde{E},\tilde{H}) = \int_{\Omega_\mathrm{f}} \tilde{H}\cdot\mathrm{curl}\tilde{E}\,\mathrm{d}x, \\ &c_\mathrm{c}(j,\tilde{E}) = \langle j, n\wedge(\tilde{E}\wedge n)_{|\Sigma}\rangle, \quad c_\mathrm{f}(j,\tilde{E}) = \langle j, n\wedge(\tilde{E}\wedge n)_{|\Sigma}\rangle. \end{aligned} \tag{14}$$

3. Design of the numerical method

3.1. Variational space discretization. The semi-discrete problem

This step is quite standard. We introduce

$$V_\mathrm{c}^h\subset V_\mathrm{c},\ W_\mathrm{c}^h\subset W_\mathrm{c},\ V_\mathrm{f}^h\subset V_\mathrm{f},\ W_\mathrm{f}^h\subset W_\mathrm{f},\ \text{and } M^h\subset M,$$

some discrete approximation subspaces of V_c, W_c, V_f, W_f, and M. In practice, these spaces will be constructed as finite element spaces associated with two different meshes of Ω_f and Ω_c: the typical situation

is that the space step in the coarse grid domain Ω_c is twice as large as in the fine grid. To the "coarse grid spaces", we associate the bilinear forms ϵ_c^h, μ_c^h, b_c^h, c_c^h defined, respectively, on $V_c^h \times V_c^h$, $W_c^h \times W_c^h$, $V_c^h \times W_c^h$ and $M^h \times V_c^h$. Each of these bilinear forms will be an "approximation" of its correspondent continuous bilinear form (without superscript h). In practice, these approximations will be related to the use of quadrature formula for the computation of the various integrals that define the bilinear forms (14).

Remark 2. Since we work with internal approximations, we could keep the continuous bilinear form instead of our approximation. However, the use of numerical integration is justified to simplify the structure of the matrices that will follow from approximation. This is particularly important for the mass lumping procedure, i.e., obtaining diagonal matrices with the bilinear forms ϵ_c and μ_c.

We proceed in the same way for the bilinear forms associated to the fine grid domain. The semi-discrete problem can be written as

Find $(E_c^h, H_c^h, E_f^h, H_f^h, J^h)$ in $V_c^h \times W_c^h \times V_f^h \times W_f^h \times M^h$ such that:

$$\begin{cases} \frac{d}{dt}\epsilon_c^h(E_c^h, \tilde{E}_c^h) - b_c^h(\tilde{E}_c^h, H_c^h) + c_c^h(J^h, \tilde{E}_c^h) = 0 & \forall \tilde{E}_c^h \in V_c^h, \\ \frac{d}{dt}\mu_c^h(H_c^h, \tilde{H}_c^h) + b_c^h(E_c^h, \tilde{H}_c^h) = 0 & \forall \tilde{H}_c^h \in W_c^h, \end{cases} \tag{15}$$

$$\begin{cases} \frac{d}{dt}\epsilon_f^h(E_f^h, \tilde{E}_f^h) - b_f^h(\tilde{E}_f^h, H_f^h) - c_f^h(J^h, \tilde{E}_f^h) = 0 & \forall \tilde{E}_f^h \in V_f^h, \\ \frac{d}{dt}\mu_f^h(H_f^h, \tilde{H}_f^h) + b_f^h(E_f^h, \tilde{H}_f^h) = 0 & \forall \tilde{H}_f^h \in W_f^h, \end{cases} \tag{16}$$

$$c_c^h(\tilde{J}^h, E_c^h) = c_f^h(\tilde{J}^h, E_f^h) \quad \forall \tilde{J}^h \in M^h. \tag{17}$$

It is useful to present the equivalent matrix formulation of problem (15)–(17). We introduce a basis of each of the discrete spaces defined above and denote by $\mathbb{E}_f$, $\mathbb{E}_c$, $\mathbb{H}_f$, $\mathbb{H}_c$ and $\mathbb{J}$ the vectors of the components of E_f^h, E_c^h, H_f^h, H_c^h and J^h in these bases (the degrees of freedom). We also define the matrices B_c, C_c, M_H^c and M_E^c by:

$$\begin{aligned} (B_c)_{j,i} &= b_c^h(v_j^c, w_i^c), \qquad 1 \leqslant i \leqslant \dim(W_c^h), \quad 1 \leqslant j \leqslant \dim(V_c^h), \\ (C_c)_{j,i} &= c_c^h(m_j, v_i^c), \qquad 1 \leqslant i \leqslant \dim(V_c^h), \quad 1 \leqslant j \leqslant \dim(M^h), \\ (M_E^c)_{i,j} &= \epsilon_c^h(v_i^c, v_j^c), \qquad 1 \leqslant i \leqslant \dim(V_c^h), \quad 1 \leqslant j \leqslant \dim(V_c^h), \\ (M_H^c)_{i,j} &= \mu_c^h(w_i^c, w_j^c), \qquad 1 \leqslant i \leqslant \dim(W_c^h), \quad 1 \leqslant j \leqslant \dim(W_c^h), \end{aligned}$$

where w_i^c (respectively, v_i^c, m_i) is the ith basis function of W_c^h (respectively, V_c^h, M^h). Matrices B_f, C_f, M_H^f and M_E^f are defined in a similar way. Finally, Problem (15)–(17) is equivalent to the following algebraic differential system:

$$\begin{cases} M_E^f \frac{d\mathbb{E}_f}{dt} - B_f\mathbb{H}_f - (C_f)^*\mathbb{J}(t) = 0, \\ M_H^f \frac{d\mathbb{H}_f}{dt} + (B_f)^*\mathbb{E}_f = 0, \\ M_E^c \frac{d\mathbb{E}_c}{dt} - B_c\mathbb{H}_c + (C_c)^*\mathbb{J}(t) = 0, \\ M_H^c \frac{d\mathbb{H}_c}{dt} + (B_c)^*\mathbb{E}_c = 0, \\ C_c\mathbb{E}_c - C_f\mathbb{E}_f = 0. \end{cases} \tag{18}$$

A condition is required to ensure the well-posedness of this system. To see that, we transform (18) into an ordinary differential system by eliminating the unknown $\mathbb{J}(t)$: we multiply the third equation of (18) by $(M_E^c)^{-1}$ and the first one by $(M_E^f)^{-1}$, taking the difference we get an expression of

$$C_{\mathrm{c}}\frac{\mathrm{d}\mathbb{E}_{\mathrm{c}}}{\mathrm{d}t}-C_{\mathrm{f}}\frac{\mathrm{d}\mathbb{E}_{\mathrm{f}}}{\mathrm{d}t},$$

as a function of $\mathbb{J}$, $\mathbb{H}_{\mathrm{f}}$ and $\mathbb{H}_{\mathrm{c}}$; because of the fifth equation of (18), this quantity must vanish, which leads to the equation

$$\Big((C_{\mathrm{c}})\big(M_E^{\mathrm{c}}\big)^{-1}(C_{\mathrm{c}})^{*}+(C_{\mathrm{f}})\big(M_E^{\mathrm{f}}\big)^{-1}(C_{\mathrm{f}})^{*}\Big)\mathbb{J}(t)=(C_{\mathrm{c}})\big(M_E^{\mathrm{f}}\big)^{-1}B_{\mathrm{c}}\mathbb{H}_{\mathrm{c}}(t)-(C_{\mathrm{f}})\big(M_E^{\mathrm{f}}\big)^{-1}B_{\mathrm{f}}\mathbb{H}_{\mathrm{f}}(t). \tag{19}$$

Thus, the existence of $\mathbb{J}$ requires that the positive symmetric matrix

$$(C_{\mathrm{c}})\big(M_E^{\mathrm{c}}\big)^{-1}(C_{\mathrm{c}})^{*}+(C_{\mathrm{f}})\big(M_E^{\mathrm{f}}\big)^{-1}(C_{\mathrm{f}})^{*}$$

is positive definite, which is equivalent to

$$\mathrm{Ker}(C_{\mathrm{f}})^{*}\cap\mathrm{Ker}(C_{\mathrm{c}})^{*}=\{0\}. \tag{20}$$

Condition (20) expresses a compatibility condition between the spaces V_{c}^h, V_{f}^h, and M^h. This condition is equivalent to an inf–sup condition, which is a well-known necessary condition for the well-posedness of a saddle point problems [5]. In our case, it reads

$$\inf_{J^h\in M^h}\sup_{(E_{\mathrm{c}}^h,E_{\mathrm{f}}^h)\in V_{\mathrm{c}}^h\times V_{\mathrm{f}}^h}\frac{c_{\mathrm{c}}^h(J^h,E_{\mathrm{c}}^h)+c_{\mathrm{c}}^h(J^h,E_{\mathrm{c}}^h)}{\|J^h\|_M\|(E_{\mathrm{c}}^h,E_{\mathrm{f}}^h)\|_{V_{\mathrm{c}}\times V_{\mathrm{f}}}}>0.$$

We will assume in what follows that (20) is satisfied.

Remark 3. Condition (20) is satisfied when one of the kernels, for instance $\mathrm{Ker}(C_{\mathrm{f}})^{*}$, is 0. We shall be in this very situation when the Yee scheme is considered in Section 4.

3.2. Time discretization

The problem is discretized with a time step Δt in the fine grid and $2\Delta t$ in the coarse grid. As is classical, in each domain, we use a staggered discretization : the electric and the magnetic fields are not computed at the same instant, but:

H_{f}^h is discretized at time step $\left(n+\frac{1}{2}\right)\Delta t\simeq H_{\mathrm{f}}^{n+\frac{1}{2}}$,
E_{f}^h is discretized at time step $n\Delta t\simeq E_{\mathrm{f}}^n$,
H_{c}^h is discretized at time step $(2n+1)\Delta t\simeq H_{\mathrm{c}}^{2n+1}$,
E_{c}^h is discretized at time step $2n\Delta t\simeq E_{\mathrm{c}}^{2n}$.

It is less obvious how to discretize the unknown J since it is defined at the interface of the two domains. We choose to discretize it with the coarse time step $2\Delta t$ at the same instant as the magnetic field in Ω_{c}:

J^h is discretized at time step $(2n+1)\Delta t\simeq J^{2n+1}$.

Finally, the discretization of (15) and (16) is performed through a standard leap frog scheme. We give below the set of equations corresponding to the interval of time $[2n\Delta t,(2n+2)\Delta t]$:

$$\begin{cases} \forall \tilde{E}_{\mathrm{f}}^h \in V_{\mathrm{f}}^h, \quad \epsilon_{\mathrm{f}}^h\left(\frac{E_{\mathrm{f}}^{2n+1}-E_{\mathrm{f}}^{2n}}{\Delta t}, \tilde{E}_{\mathrm{f}}^h\right) - b_{\mathrm{f}}^h\left(\tilde{E}_{\mathrm{f}}^h, H_{\mathrm{f}}^{2n+\frac{1}{2}}\right) = c_{\mathrm{f}}^h\left(J^{2n+1}, \tilde{E}_{\mathrm{f}}^h\right), \\ \forall \tilde{H}_{\mathrm{f}}^h \in W_{\mathrm{f}}^h, \quad \mu_{\mathrm{f}}^h\left(\frac{H_{\mathrm{f}}^{2n+\frac{1}{2}}-H_{\mathrm{f}}^{2n-\frac{1}{2}}}{\Delta t}, \tilde{H}_{\mathrm{f}}^h\right) + b_{\mathrm{f}}^h\left(E_{\mathrm{f}}^{2n}, \tilde{H}_{\mathrm{f}}^h\right) = 0, \end{cases}$$
$$\begin{cases} \forall \tilde{E}_{\mathrm{f}}^h \in V_{\mathrm{f}}^h, \quad \epsilon_{\mathrm{f}}^h\left(\frac{E_{\mathrm{f}}^{2n+2}-E_{\mathrm{f}}^{2n+1}}{\Delta t}, \tilde{E}_{\mathrm{f}}^h\right) - b_{\mathrm{f}}^h\left(\tilde{E}_{\mathrm{f}}^h, H_{\mathrm{f}}^{2n+\frac{3}{2}}\right) = c_{\mathrm{f}}^h\left(J^{2n+1}, \tilde{E}_{\mathrm{f}}^h\right), \\ \forall \tilde{H}_{\mathrm{f}}^h \in W_{\mathrm{f}}^h, \quad \mu_{\mathrm{f}}^h\left(\frac{H_{\mathrm{f}}^{2n+\frac{3}{2}}-H_{\mathrm{f}}^{2n+\frac{1}{2}}}{\Delta t}, \tilde{H}_{\mathrm{f}}^h\right) + b_{\mathrm{f}}^h\left(E_{\mathrm{f}}^{2n+1}, \tilde{H}_{\mathrm{f}}^h\right) = 0, \end{cases} \tag{21}$$

$$\begin{cases} \forall \tilde{E}_{\mathrm{c}}^h \in V_{\mathrm{c}}^h, \quad \epsilon_{\mathrm{c}}^h\left(\frac{E_{\mathrm{c}}^{2n+2}-E_{\mathrm{c}}^{2n}}{2\Delta t}, \tilde{E}_{\mathrm{c}}^h\right) - b_{\mathrm{c}}^h\left(\tilde{E}_{\mathrm{c}}^h, H_{\mathrm{c}}^{2n+1}\right) = -c_{\mathrm{c}}^h\left(J^{2n+1}, \tilde{E}_{\mathrm{c}}^h\right), \\ \forall \tilde{H}_{\mathrm{c}}^h \in W_{\mathrm{c}}^h, \quad \mu_{\mathrm{c}}^h\left(\frac{H_{\mathrm{c}}^{2n+1}-H_{\mathrm{c}}^{2n-1}}{2\Delta t}, \tilde{H}_{\mathrm{c}}^h\right) + b_{\mathrm{c}}^h\left(E_{\mathrm{c}}^{2n}, \tilde{H}_{\mathrm{c}}^h\right) = 0. \end{cases} \tag{22}$$

Only the constraint remains to be discretized. We do not choose it in just any way, but we use a time centered average, adequately selected to lead to a conservative scheme (as it will be seen afterward). This is the key point of our method. This scheme reads

$$\forall J'^h \in \mathscr{M}_h, \quad c_{\mathrm{f}}^h\left(J'^h, \frac{E_{\mathrm{f}}^{2n+2}+2E_{\mathrm{f}}^{2n+1}+E_{\mathrm{f}}^{2n}}{4}\right) = c_{\mathrm{c}}^h\left(J'^h, \frac{E_{\mathrm{c}}^{2n+2}+E_{\mathrm{c}}^{2n}}{2}\right). \tag{23}$$

The matrix form of this system is:

$$\begin{cases} \begin{cases} M_E^{\mathrm{f}} \frac{\mathbb{E}_{\mathrm{f}}^{2n+1}-\mathbb{E}_{\mathrm{f}}^{2n}}{\Delta t} - B_{\mathrm{f}}\mathbb{H}_{\mathrm{f}}^{2n+\frac{1}{2}} - (C_{\mathrm{f}})^*\mathbb{J}^{2n+1} = 0, & (1) \\ M_H^{\mathrm{f}} \frac{\mathbb{H}_{\mathrm{f}}^{2n+\frac{1}{2}}-\mathbb{H}_{\mathrm{f}}^{2n-\frac{1}{2}}}{\Delta t} + (B_{\mathrm{f}})^*\mathbb{E}_{\mathrm{f}}^{2n} = 0, & (2) \\ M_E^{\mathrm{f}} \frac{\mathbb{E}_{\mathrm{f}}^{2n+2}-\mathbb{E}_{\mathrm{f}}^{2n+1}}{\Delta t} - B_{\mathrm{f}}\mathbb{H}_{\mathrm{f}}^{2n+\frac{3}{2}} - (C_{\mathrm{f}})^*\mathbb{J}^{2n+1} = 0, & (3) \\ M_H^{\mathrm{f}} \frac{\mathbb{H}_{\mathrm{f}}^{2n+\frac{3}{2}}-\mathbb{H}_{\mathrm{f}}^{2n+\frac{1}{2}}}{\Delta t} + (B_{\mathrm{f}})^*\mathbb{E}_{\mathrm{f}}^{2n+1} = 0, & (4) \end{cases} \\ \begin{cases} M_E^{\mathrm{c}} \frac{\mathbb{E}_{\mathrm{c}}^{2n+2}-\mathbb{E}_{\mathrm{c}}^{2n}}{2\Delta t} - B_{\mathrm{c}}\mathbb{H}_{\mathrm{c}}^{2n+1} + (C_{\mathrm{c}})^*\mathbb{J}^{2n+1} = 0, & (5) \\ M_H^{\mathrm{c}} \frac{\mathbb{H}_{\mathrm{c}}^{2n+1}-\mathbb{H}_{\mathrm{c}}^{2n-1}}{2\Delta t} + (B_{\mathrm{c}})^*\mathbb{E}_{\mathrm{c}}^{2n} = 0, & (6) \end{cases} \\ C_{\mathrm{c}} \frac{\mathbb{E}_{\mathrm{c}}^{2n+2}+\mathbb{E}_{\mathrm{c}}^{2n}}{2} - C_{\mathrm{f}} \frac{\mathbb{E}_{\mathrm{f}}^{2n+2}+2\mathbb{E}_{\mathrm{f}}^{2n+1}+\mathbb{E}_{\mathrm{f}}^{2n}}{4} = 0. \quad (7) \end{cases} \tag{24}$$

This system, initialized by the discrete fields $\mathbb{E}_{\mathrm{f}}^0$, $\mathbb{E}_{\mathrm{c}}^0$, $\mathbb{H}_{\mathrm{f}}^{1/2}$ and $\mathbb{H}_{\mathrm{c}}^1$, allows us to compute the solutions from time step $2n$ to time step $2n + 2$.

3.3. Theoretical analysis of the fully discrete scheme

3.3.1. Existence and calculation of the discrete solution

In this section, we show how to compute the solution of our scheme. A simple look at the system shows that if the current is known, all the other unknowns can be computed explicitly (the current plays then the role of a source term): the existence and uniqueness of the discrete solution is a simple consequence of the existence of J^{2n+1}. So, we just have to show how the unknown J can be computed.

We assume here that the discrete solution is known up to time step t^{2n}. We show below that for each n, $\mathbb{J}^{2n+1}$ is obtained by solving a symmetric positive linear system.

We first take the difference between the first and the third equation of (24). This permits us to eliminate the current and leads to

$$M_E^{\mathrm{f}} \frac{\mathbb{E}_{\mathrm{f}}^{2n+2} - 2\mathbb{E}_{\mathrm{f}}^{2n+1} + \mathbb{E}_{\mathrm{f}}^{2n}}{\Delta t^2} - B_{\mathrm{f}} \frac{\mathbb{H}_{\mathrm{f}}^{2n+\frac{1}{2}} - \mathbb{H}_{\mathrm{f}}^{2n-\frac{1}{2}}}{\Delta t} = 0. \tag{25}$$

From the second equation of (24), we have

$$M_E^{\mathrm{f}} \frac{\mathbb{E}_{\mathrm{f}}^{2n+2} - 2\mathbb{E}_{\mathrm{f}}^{2n+1} + \mathbb{E}_{\mathrm{f}}^{2n}}{\Delta t^2} + B_{\mathrm{f}} \left(M_H^{\mathrm{f}}\right)^{-1} (B_{\mathrm{f}})^* \mathbb{E}_{\mathrm{f}}^{2n+1} = 0, \tag{26}$$

and therefore,

$$\frac{\mathbb{E}_{\mathrm{f}}^{2n+2} + 2\mathbb{E}_{\mathrm{f}}^{2n+1} + \mathbb{E}_{\mathrm{f}}^{2n}}{4} = \left(Id - \frac{\Delta t^2}{4} \left(M_E^{\mathrm{f}}\right)^{-1} B_{\mathrm{f}} \left(M_H^{\mathrm{f}}\right)^{-1} (B_{\mathrm{f}})^* \right) \mathbb{E}_{\mathrm{f}}^{2n+1}. \tag{27}$$

The first equation of (24) is used to get

$$M_E^{\mathrm{f}} \mathbb{E}_{\mathrm{f}}^{2n+1} = \mathbb{T}_{\mathrm{f}}^{2n+1} + (C_{\mathrm{f}})^* \mathbb{J}^{2n+1}, \tag{28}$$

where $\mathbb{T}_{\mathrm{f}}^{2n+1}$ depends only on $\mathbb{E}_{\mathrm{f}}^{2n}$, $\mathbb{H}_{\mathrm{f}}^{2n+1}$. Since $\mathbb{H}_{\mathrm{f}}^{2n+1}$ is given explicitly in the sixth equation of (24), $\mathbb{T}_{\mathrm{f}}^{2n+1}$ is known. Finally, introducing the symmetric matrix,

$$A_{\mathrm{f}} = \left(\left(M_E^{\mathrm{f}}\right)^{-1} - \frac{\Delta t^2}{4} \left(M_E^{\mathrm{f}}\right)^{-1} B_{\mathrm{f}} \left(M_H^{\mathrm{f}}\right)^{-1} (B_{\mathrm{f}})^* \left(M_E^{\mathrm{f}}\right)^{-1} \right), \tag{29}$$

we have

$$\frac{\mathbb{E}_{\mathrm{f}}^{2n+2} + 2\mathbb{E}_{\mathrm{f}}^{2n+1} + \mathbb{E}_{\mathrm{f}}^{2n}}{4} = A_{\mathrm{f}} \left(\mathbb{T}_{\mathrm{f}}^{2n+1} + (C_{\mathrm{f}})^* \mathbb{J}^{2n+1} \right). \tag{30}$$

Proceeding in the same way, with (24).(5), we get,

$$\frac{\mathbb{E}_{\mathrm{c}}^{2n+2} + \mathbb{E}_{\mathrm{c}}^{2n}}{2} = \mathbb{T}_{\mathrm{c}}^{2n+1} - \left(M_E^{\mathrm{c}}\right)^{-1} (C_{\mathrm{c}})^* \mathbb{J}^{2n+1}, \tag{31}$$

where, once again, $\mathbb{T}_{\mathrm{c}}^{2n+1}$ is function of known quantities, independent of $\mathbb{J}^{2n+1}$. Substituting (31) and (30) in (24).(7), we obtain:

$$\begin{cases} Q\mathbb{J}^{2n+1}(t) = (C_{\mathrm{c}})\mathbb{T}_{\mathrm{c}}^{2n+1} - (C_{\mathrm{f}})A_{\mathrm{f}}\mathbb{T}_{\mathrm{f}}^{2n+1}. \\ Q = \left((C_{\mathrm{c}}) \left(M_E^{\mathrm{c}}\right)^{-1} (C_{\mathrm{c}})^* + (C_{\mathrm{f}})A_{\mathrm{f}}(C_{\mathrm{f}})^* \right). \end{cases} \tag{32}$$

We notice that this linear system is invertible as long as:

$$\begin{cases} \mathrm{Ker}(C_{\mathrm{f}})^* \cap \mathrm{Ker}(C_{\mathrm{c}})^* = \{0\}, \\ A_{\mathrm{f}} > 0 : \quad \frac{\Delta t^2}{4} B_{\mathrm{f}} \left(M_H^{\mathrm{f}}\right)^{-1} (B_{\mathrm{f}})^* < M_E^{\mathrm{f}}, \end{cases} \tag{33}$$

where the inequalities between symmetric matrices have to be taken in the sense of the associated quadratic form. The first condition was already introduced to ensure the well-posedness of the semi-discretized problem. The second condition implies a bound for the time step Δt; if $\mathscr{B}_{\mathrm{f}}^h$ is the linear operator from V_{f}^h to W_{f}^h defined by the formula (44) associated with the matrix $(M_H^{\mathrm{f}})^{-1}(B_{\mathrm{f}}^h)^*$, the condition is

$$\frac{\Delta t^2}{4} \mu_{\mathrm{f}}^h \left(\mathscr{B}_h \tilde{E}, \mathscr{B}_h \tilde{E} \right) \leqslant \epsilon_{\mathrm{f}}^h \left(\tilde{E}, \tilde{E} \right) \quad \forall \tilde{E} \in V_h^{\mathrm{f}}.$$

We shall see later that this condition coincides with the stability condition of the scheme.

3.3.2. Energy estimation and stability

We intend to show the stability of our scheme through the conservation of an appropriate energy. This is the key point of the analysis that justifies the choice of the coupling scheme (23). More precisely, we show the conservation between two coarse time steps of a quadratic quantity that appears to be a discrete equivalent of the electro-magnetic energy, namely, if

$$\mathscr{E}_{\mathrm{T}}^{2n} = \tfrac{1}{2}\epsilon_{\mathrm{c}}^{h}(E_{\mathrm{c}}^{2n}, E_{\mathrm{c}}^{2n}) + \tfrac{1}{2}\mu_{\mathrm{c}}^{h}(H_{\mathrm{c}}^{2n+1}, H_{\mathrm{c}}^{2n-1}) + \tfrac{1}{2}\epsilon_{\mathrm{f}}^{h}(E_{\mathrm{f}}^{2n}, E_{\mathrm{f}}^{2n}) + \tfrac{1}{2}\mu_{\mathrm{f}}^{h}(H_{\mathrm{f}}^{2n+\frac{1}{2}}, H_{\mathrm{f}}^{2n-\frac{1}{2}}), \tag{34}$$

then the following equality holds:

$$\mathscr{E}_{\mathrm{T}}^{2n} = \mathscr{E}_{\mathrm{T}}^{0} \quad \forall n \geqslant 0. \tag{35}$$

We then show that this conservation implies the L^2 stability of the scheme provided that a stability condition (CFL condition) is satisfied.

Taking $\tilde{E}_{\mathrm{c}}^{h} = \frac{E_{\mathrm{c}}^{2n+2}+E_{\mathrm{c}}^{2n}}{2}$ in (22), we obtain

$$\epsilon_{\mathrm{c}}^{h}\left(\frac{E_{\mathrm{c}}^{2n+2}-E_{\mathrm{c}}^{2n}}{2\Delta t}, \frac{E_{\mathrm{c}}^{2n+2}+E_{\mathrm{c}}^{2n}}{2}\right) - b_{\mathrm{c}}^{h}\left(\frac{E_{\mathrm{c}}^{2n+2}+E_{\mathrm{c}}^{2n}}{2}, H_{\mathrm{c}}^{2n+1}\right) = -c_{\mathrm{c}}^{h}\left(J^{2n+1}, \frac{E_{\mathrm{c}}^{2n+2}+E_{\mathrm{c}}^{2n}}{2}\right). \tag{36}$$

From (22) written at two consecutive time steps, we also deduce

$$\forall \tilde{H}_{\mathrm{c}}^{h} \in W_{\mathrm{c}}^{h}, \quad \mu_{\mathrm{c}}^{h}\left(\frac{H_{\mathrm{c}}^{2n+3}-H_{\mathrm{c}}^{2n-1}}{4\Delta t}, \tilde{H}_{\mathrm{c}}^{h}\right) + b_{\mathrm{c}}^{h}\left(\frac{E_{\mathrm{c}}^{2n+2}+E_{\mathrm{c}}^{2n}}{2}, \tilde{H}_{\mathrm{c}}^{h}\right) = 0.$$

Therefore, taking $\tilde{H}_{\mathrm{c}}^{h} = H_{\mathrm{c}}^{2n+1}$, we get

$$\mu_{\mathrm{c}}^{h}\left(\frac{H_{\mathrm{c}}^{2n+3}-H_{\mathrm{c}}^{2n-1}}{4\Delta t}, H_{\mathrm{c}}^{2n+1}\right) + b_{\mathrm{c}}^{h}\left(\frac{E_{\mathrm{c}}^{2n+2}+E_{\mathrm{c}}^{2n}}{2}, H_{\mathrm{c}}^{2n+1}\right) = 0. \tag{37}$$

Let us define the coarse grid energy at time step $2n$,

$$\mathscr{E}_{\mathrm{c}}^{2n} = \tfrac{1}{2}\epsilon_{\mathrm{c}}^{h}(E_{\mathrm{c}}^{2n}, E_{\mathrm{c}}^{2n}) + \tfrac{1}{2}\mu_{\mathrm{c}}^{h}(H_{\mathrm{c}}^{2n+1}, H_{\mathrm{c}}^{2n-1}).$$

Adding Eqs. (37) and (36) leads to the identity

$$\frac{\mathscr{E}_{\mathrm{c}}^{2n+2}-\mathscr{E}_{\mathrm{c}}^{2n}}{2\Delta t} = -c_{\mathrm{c}}^{h}\left(J^{2n+1}, \frac{E^{2n+2}+E^{2n}}{2}\right). \tag{38}$$

In the same way, if we introduce the fine grid energy at time step n,

$$\mathscr{E}_{\mathrm{f}}^{n} = \tfrac{1}{2}\epsilon_{\mathrm{f}}^{h}(E_{\mathrm{f}}^{n}, E_{\mathrm{f}}^{n}) + \tfrac{1}{2}\mu_{\mathrm{f}}^{h}(H_{\mathrm{f}}^{n+\frac{1}{2}}, H_{\mathrm{f}}^{n-\frac{1}{2}}), \tag{39}$$

we easily obtain the two equalities:

$$\frac{\mathscr{E}_{\mathrm{f}}^{2n+1}-\mathscr{E}_{\mathrm{f}}^{2n}}{\Delta t} = c_{\mathrm{f}}^{h}\left(J^{2n+1}, \frac{E_{\mathrm{f}}^{2n+1}+E_{\mathrm{f}}^{2n}}{2}\right),$$
$$\frac{\mathscr{E}_{\mathrm{f}}^{2n+2}-\mathscr{E}_{\mathrm{f}}^{2n+1}}{\Delta t} = c_{\mathrm{f}}^{h}\left(J^{2n+1}, \frac{E_{\mathrm{f}}^{2n+2}+E_{\mathrm{f}}^{2n+1}}{2}\right),$$

from which we deduce

$$\frac{\mathscr{E}_{\mathrm{f}}^{2n+2}-\mathscr{E}_{\mathrm{f}}^{2n}}{2\Delta t} = c_{\mathrm{f}}^{h}\left(J^{2n+1}, \frac{E_{\mathrm{f}}^{2n+2}+2E_{\mathrm{f}}^{2n+1}+E_{\mathrm{f}}^{2n}}{4}\right). \tag{40}$$

Let us define the total energy at time step $2n$ as

$$\mathscr{E}_{\mathrm{T}}^{2n} = \mathscr{E}_{\mathrm{f}}^{2n} + \mathscr{E}_{\mathrm{c}}^{2n}.$$

We get from (40) and (38)

$$\frac{\mathscr{E}_{\mathrm{T}}^{2n+2} - \mathscr{E}_{\mathrm{T}}^{2n}}{2\Delta t} = c_{\mathrm{f}}^{h}\left(J^{2n+1}, \frac{E_{\mathrm{f}}^{2n+2} + 2E_{\mathrm{f}}^{2n+1} + E_{\mathrm{f}}^{2n}}{4}\right) - c_{\mathrm{c}}^{h}\left(J^{2n+1}, \frac{E_{\mathrm{c}}^{2n+2} + E_{\mathrm{c}}^{2n}}{2}\right). \tag{41}$$

The right hand side of (41) vanishes which implies the conservation property $\mathscr{E}_{\mathrm{T}}^{2n+2} = \mathscr{E}_{\mathrm{T}}^{2n}$, whence (35).

Remark 4. The total energy $\mathscr{E}_{\mathrm{T}}^{2n}$ is a discrete equivalent of the electro-magnetic energy

$$\int_{\Omega} \left(\epsilon_0 E^2(x,t) + \mu_0 H^2(x,t)\right) \mathrm{d}x.$$

Identity (35) shows that the coupling scheme is exactly the one that preserves the energy $\mathscr{E}_{\mathrm{T}}^{2n}$.

From the conservation of the discrete energy, it is possible, if not easy, to find a sufficient condition of stability. The idea is to find a sufficient condition for having a true energy (that is a positive definite quadratic form). The trick is to use the remarkable identity

$$\mu_{\mathrm{f}}^{h}(H_{\mathrm{f}}^{n+\frac{1}{2}}, H_{\mathrm{f}}^{n-\frac{1}{2}}) = \mu_{\mathrm{f}}^{h}\left(\frac{H_{\mathrm{f}}^{n+\frac{1}{2}} + H_{\mathrm{f}}^{n-\frac{1}{2}}}{2}, \frac{H_{\mathrm{f}}^{n+\frac{1}{2}} + H_{\mathrm{f}}^{n-\frac{1}{2}}}{2}\right) - \frac{\Delta t^2}{4}\mu_{\mathrm{f}}^{h}\left(\frac{H_{\mathrm{f}}^{n+\frac{1}{2}} - H_{\mathrm{f}}^{n-\frac{1}{2}}}{\Delta t}, \frac{H_{\mathrm{f}}^{n+\frac{1}{2}} - H_{\mathrm{f}}^{n-\frac{1}{2}}}{\Delta t}\right) \tag{42}$$

and to estimate the negative term in (42) with the help of $\epsilon_{\mathrm{f}}^{h}(E_{\mathrm{f}}^{n}, E_{\mathrm{f}}^{n})$.

More precisely, the second equation of (21) reads

$$\frac{H_{\mathrm{f}}^{n+\frac{1}{2}} - H_{\mathrm{f}}^{n-\frac{1}{2}}}{\Delta t} = \mathscr{B}_{\mathrm{f}}^{h} E_{\mathrm{f}}^{n}, \tag{43}$$

where $\mathscr{B}_{\mathrm{f}}^{h}$ is the operator from V_{f}^{h} into W_{f}^{h} defined by

$$\mu_{\mathrm{f}}^{h}\left(\mathscr{B}_{\mathrm{f}}^{h} v_{\mathrm{f}}^{h}, w_{\mathrm{f}}^{h}\right) = b_{\mathrm{f}}^{h}(v_{\mathrm{f}}^{h}, w_{\mathrm{f}}^{h}) \quad \forall w_{\mathrm{f}}^{h} \in W_{\mathrm{f}}^{h} \tag{44}$$

with norm β_{f}

$$\beta_{\mathrm{f}}^2 = \sup_{\tilde{E} \in V_{\mathrm{f}}^{h}} \frac{\mu_{\mathrm{f}}^{h}\left(\mathscr{B}_{\mathrm{f}}^{h}\tilde{E}, \mathscr{B}_{\mathrm{f}}^{h}\tilde{E}\right)}{\epsilon_{\mathrm{f}}^{h}(\tilde{E}, \tilde{E})}. \tag{45}$$

Using (43) in (42) as well as (45) provides the bound

$$\mu_{\mathrm{f}}^{h}(H_{\mathrm{f}}^{n+\frac{1}{2}}, H_{\mathrm{f}}^{n-\frac{1}{2}}) \geqslant \mu_{\mathrm{f}}^{h}\left(\frac{H_{\mathrm{f}}^{n+\frac{1}{2}} + H_{\mathrm{f}}^{n-\frac{1}{2}}}{2}, \frac{H_{\mathrm{f}}^{n+\frac{1}{2}} + H_{\mathrm{f}}^{n-\frac{1}{2}}}{2}\right) - \frac{\beta_{\mathrm{f}}^2 \Delta t^2}{4}\epsilon_{\mathrm{f}}^{h}(E_{\mathrm{f}}^{n}, E_{\mathrm{f}}^{n}) \tag{46}$$

which, substituted into the expression of the fine grid energy (39), leads to

$$\frac{1}{2}\left(1 - \frac{\beta_{\mathrm{f}}^2 \Delta t^2}{4}\right)\epsilon_{\mathrm{f}}^{h}(E_{\mathrm{f}}^{n}, E_{\mathrm{f}}^{n}) + \frac{1}{2}\mu_{\mathrm{f}}^{h}\left(\frac{H_{\mathrm{f}}^{n+\frac{1}{2}} + H_{\mathrm{f}}^{n-\frac{1}{2}}}{2}, \frac{H_{\mathrm{f}}^{n+\frac{1}{2}} + H_{\mathrm{f}}^{n-\frac{1}{2}}}{2}\right) \leqslant \mathscr{E}_{\mathrm{f}}^{n}. \tag{47}$$

We can of course proceed in a similar way for the coarse grid. We introduce the operator $\mathscr{B}_{\mathrm{c}}^{h}$ and its norm β_{c}^{h}, obtaining

$$\frac{1}{2}\left(1 - \frac{\beta_{\mathrm{c}}^2 (2\Delta t)^2}{4}\right)\epsilon_{\mathrm{c}}^{h}(E_{\mathrm{c}}^{2n}, E_{\mathrm{c}}^{2n}) + \frac{1}{2}\mu_{\mathrm{c}}^{h}\left(\frac{H_{\mathrm{c}}^{2n+1} + H_{\mathrm{c}}^{2n-1}}{2}, \frac{H_{\mathrm{c}}^{2n+1} + H_{\mathrm{c}}^{2n-1}}{2}\right) \leqslant \mathscr{E}_{\mathrm{c}}^{2n}. \tag{48}$$

Gathering the two estimates, we get

$$\left(1-\beta_c^2\Delta t^2\right)\epsilon_c^h(E_c^{2n},E_c^{2n})+\mu_c^h\left(\frac{H_c^{2n+1}+H_c^{2n-1}}{2},\frac{H_c^{2n+1}+H_c^{2n-1}}{2}\right)+\left(1-\frac{\beta_f^2\Delta t^2}{4}\right)\epsilon_f^h(E_f^{2n},E_f^{2n})$$
$$+\mu_f^h\left(\frac{H_f^{2n+\frac{1}{2}}+H_f^{2n-\frac{1}{2}}}{2},\frac{H_f^{2n+\frac{1}{2}}+H_f^{2n-\frac{1}{2}}}{2}\right)\leqslant 2\mathscr{E}_f^{2n}+2\mathscr{E}_c^{2n}=2\mathscr{E}_T^{2n}=2\mathscr{E}_T^0. \tag{49}$$

The last equality coming from the conservation of the total energy.

Let us assume

$$\Delta t<\frac{2}{\beta_f}\quad\text{and}\quad\Delta t<\frac{1}{\beta_c}. \tag{50}$$

Every term in the left hand side of the inequality in (49) is positive and the norms of the solutions are estimated independently of the steps Δt and h. More precisely, inequality (49) directly provides L^2 estimates of both

$$E_f^{2n}\quad\text{and}\quad\frac{H_f^{2n+\frac{1}{2}}+H_f^{2n-\frac{1}{2}}}{2}.$$

Using (43) at times $2n$ as well as the CFL condition permits us to estimate separately $H_f^{2n+\frac{1}{2}}$ and $H_f^{2n-\frac{1}{2}}$. We proceed along the same lines in the coarse grid to estimate H_c^{2n+1}. It remains to estimate E_f^{2n+1}, that can be done through (26) as in [2]. We deduce the stability of the coupled scheme under the CFL condition (50).

4. Application to the Yee scheme

In this section, we apply the abstract framework of the previous section to a special case, in order the design of a mesh refinement method for the Yee scheme. Let us consider a regular grid of $\mathbb{R}^3$ with cubes of size $2h$. We assume that the domain Ω_f is a subset of cubes of this grid. We define a refined grid of discretization on Ω_f by dividing each cube in Ω_f into eight identical cubes of side length h. In this way, we produce a fine grid in Ω_f and a coarse grid in Ω_c; the set of cubes of size h in Ω_f will be denoted by $\mathscr{T}_h$ and the set of cubes of size $2h$ covering Ω_c will be $\mathscr{T}_{2h}$.

4.1. Discretization spaces for the electro-magnetic field

For the discretization of the electric field, the Ndec's first order edge element is chosen, namely:

$$\begin{aligned}V_c^h&=\left\{E_c^h\in V_c/\forall K\in\mathscr{T}_{2h},\ E_c^h|_K\in\mathscr{Q}_{0,1,1}\times\mathscr{Q}_{1,0,1}\times\mathscr{Q}_{1,1,0}\right\},\\ V_f^h&=\left\{E_f^h\in V_f/\forall K\in\mathscr{T}_h,\ E_f^h|_K\in\mathscr{Q}_{0,1,1}\times\mathscr{Q}_{1,0,1}\times\mathscr{Q}_{1,1,0}\right\},\end{aligned} \tag{51}$$

where $\mathscr{Q}_{p1,p2,p3}$ denotes the set of polynomials whose degree in the variable x_j is less or equal to p_j. It is well known that each vector field E_f^h in V_f^h is entirely determined by the knowledge of the circulations along the edges e_k^f of the mesh $\mathscr{T}_h$. These are the degrees of freedom of the finite element space V_f^h, and the basis functions associated to them are denoted v_k^f. The same holds for the coarse grid. For the magnetic field, we shall use $H(\mathrm{div},\Omega_c)$ and $H(\mathrm{div},\Omega_f)$ face elements, i.e.:

$$\begin{aligned}W_c^h&=\left\{H_c^h\in W_c/\forall K\in\mathscr{T}_{2h},\ H_c^h|_K\in\mathscr{Q}_{1,0,0}\times\mathscr{Q}_{0,1,0}\times\mathscr{Q}_{0,0,1}\right\},\\ W_f^h&=\left\{H_f^h\in W_f/\forall K\in\mathscr{T}_h,\ H_f^h|_K\in\mathscr{Q}_{1,0,0}\times\mathscr{Q}_{0,1,0}\times\mathscr{Q}_{0,0,1}\right\}.\end{aligned} \tag{52}$$

Any vector field H_{f}^h in W_{f}^h is entirely determined by the knowledge of their fluxes across the faces F_ℓ^{f} of the mesh $\mathscr{T}_h$. These are the degrees of freedom of the finite element space V_{f}^h, and the basis functions associated to them are denoted w_ℓ^{f}. The same holds for the coarse grid.

For defining the approximate bilinear forms, we introduce a quadrature formula. Let φ be a function defined in Ω_{f} (respectively, Ω_{c}) such that the restriction to each cube K of $\mathscr{T}_h$ (respectively, $\mathscr{T}_{2h}$) is continuous in K, we define the discrete integral

$$\fint_{\Omega_f} \varphi(x)\,\mathrm{d}x = \sum_{K\in\mathscr{T}^h} \frac{\mathrm{meas}(K)}{8} \sum_{\ell=1}^{8} \varphi_{|K}(S_\ell^K), \quad \fint_{\Omega_c} \varphi(x)\,\mathrm{d}x = \sum_{K\in\mathscr{T}^{2h}} \frac{\mathrm{meas}(K)}{8} \sum_{\ell=1}^{8} \varphi_{|K}(S_\ell^K), \tag{53}$$

where $(S_\ell^K)_{\ell=1,8}$ is the set of the vertices of K, and:

$$\begin{aligned}
&\epsilon_{\mathrm{c}}^h(\tilde{E},\tilde{E}) = \fint_{\Omega_c} \epsilon_0 \tilde{E}\cdot\tilde{E}\,\mathrm{d}x, \quad \epsilon_{\mathrm{f}}^h(\tilde{E},\tilde{E}) = \fint_{\Omega_f} \epsilon_0 \tilde{E}\cdot\tilde{E}\,\mathrm{d}x,\\
&\mu_{\mathrm{c}}^h(\tilde{H},\tilde{H}) = \fint_{\Omega_c} \mu_0 \tilde{H}\cdot\tilde{H}\,\mathrm{d}x, \quad \mu_{\mathrm{f}}^h(\tilde{H},\tilde{H}) = \fint_{\Omega_f} \mu_0 \tilde{H}\cdot\tilde{H}\,\mathrm{d}x,\\
&b_{\mathrm{c}}^h(\tilde{E},\tilde{H}) = \fint_{\Omega_c} \tilde{H}\cdot\mathrm{curl}\tilde{E}\,\mathrm{d}x, \quad b_{\mathrm{f}}^h(\tilde{E},\tilde{H}) = \fint_{\Omega_f} \tilde{H}\cdot\mathrm{curl}\tilde{E}\,\mathrm{d}x.
\end{aligned} \tag{54}$$

These quadrature formulae allow us to obtain diagonal mass matrices: we have (δ_i^j is the Kronecker symbol):

$$\begin{aligned}
&\left(M_E^{\mathrm{f}}\right)_{k,k'} = \delta_k^{k'} \frac{\epsilon_0 h}{4} \#\{K\in\mathscr{T}_h / e_k^{\mathrm{f}} \subset K\}, \quad \left(M_E^{\mathrm{c}}\right)_{i,i'} = \delta_i^{i'} \frac{2h\epsilon_0}{4} \#\{K\in\mathscr{T}_{2h} / e_i^{\mathrm{c}} \subset K\},\\
&\left(M_H^{\mathrm{f}}\right)_{\ell,\ell'} = \delta_\ell^{\ell'} \frac{\mu_0}{2h} \#\{K\in\mathscr{T}_h / F_\ell^{\mathrm{f}} \subset K\}, \quad \left(M_H^{\mathrm{c}}\right)_{m,m'} = \delta_m^{m'} \frac{\mu_0}{4h} \#\{K\in\mathscr{T}_{2h} / F_m^{\mathrm{c}} \subset K\}.
\end{aligned}$$

To construct the matrices B_{f}^h and B_{c}^h, it is useful to notice that

$$\frac{1}{\mu_0}\mathrm{curl} V_{\mathrm{f}}^h \subset W_{\mathrm{f}}^h, \quad \frac{1}{\mu_0}\mathrm{curl} V_{\mathrm{c}}^h \subset W_{\mathrm{c}}^h \tag{55}$$

and consequently

$$B_{\mathrm{f}} = \frac{1}{\mu_0} M_H^{\mathrm{f}} \mathrm{curl}^{\mathrm{f}}, \quad B_{\mathrm{c}} = \frac{1}{\mu_0} M_H^{\mathrm{c}} \mathrm{curl}^{\mathrm{c}}, \tag{56}$$

where the matrices $\mathrm{curl}^{\mathrm{f}}$ and $\mathrm{curl}^{\mathrm{c}}$ are defined through

$$\mathrm{curl} v_k^{\mathrm{f}}(x) = \sum_{\ell / e_k^{\mathrm{f}} \subset F_\ell^{\mathrm{f}} \in \mathscr{T}_h} \left(\mathrm{curl}^{\mathrm{f}}\right)_{\ell,k} w_\ell^{\mathrm{f}}(x), \quad \mathrm{curl} v_i^{\mathrm{c}}(x) = \sum_{m / e_i^{\mathrm{c}} \subset F_m^{\mathrm{c}} \in \mathscr{T}_{2h}} \left(\mathrm{curl}^{\mathrm{c}}\right)_{m,i} w_m^{\mathrm{c}}(x). \tag{57}$$

Both matrices ($\mathrm{curl}^{\mathrm{f}}$) and ($\mathrm{curl}^{\mathrm{c}}$) have at most four non-zero elements per line: at most two values are 1 while two others are -1, the signs being determined according to the relative orientation of the edge with respect to the face. The lines with less than four non-zero elements correspond to faces situated on the boundary of the domains Ω_{f} or Ω_{c}.

It is not difficult (and classical) to check that our discretization procedure leads to the Yee scheme [15] as the inner scheme in both the fine and the coarse grids (it simply amounts to transform the degrees of freedom of the solution into field values by an appropriate scaling).

4.2. Discretization space for the current

For the discretization of the current J, we construct a surface mesh of the interface Σ as the trace of the coarse grid in Ω_{c}. This mesh is made of the faces (squares of side length $2h$) of the cubes of the coarse grid

that intersect Σ. Let us denote by $\mathscr{T}_{2h}(\Sigma)$ the set of these faces. As for boundary element methods, it is natural to choose the Rao–Wilson–Glisson (RWG) elements to construct the discretization space M^h

$$M^h = \left\{ J^h \in M / \forall F \in \mathscr{T}_{2h}(\Sigma), \quad J^h_{|F} \in \mathscr{Q}_{1,0} \times \mathscr{Q}_{0,1} \right\}. \tag{58}$$

More precisely:

- For each face F, $J^h_{|F}$ is tangent to F.
- Let (u_1,u_2) be an orthonormal basis, made of two unit vectors parallel to the edges of the face F, and (y_1,y_2) the corresponding tangential coordinates. Then, $J^h_{|F} \in \mathscr{Q}_{1,0} \times \mathscr{Q}_{0,1}$ means that $J^h_{|F} \cdot u_1$ is a polynomial of degree one with respect to y_1 and constant in y_2 while $J^h_{|F} \cdot u_2$ is a polynomial of degree one with respect to y_2 and constant in y_1.
- In addition, there is one condition per edge of the mesh, namely the continuity of the normal flux. In practice, to any edge e^{c}_j of $\mathscr{T}_{2h}(\Sigma)$ we associate a unit vector n_j that defines an orientation for the fluxes across e^{c}_j. This permits us to define without ambiguity $F^{\mathrm{c}}_{j,+}$ and $F^{\mathrm{c}}_{j,-}$ as the two faces adjacent to e^{c}_j (n_j is outgoing for $F^{\mathrm{c}}_{j,+}$, incoming for $F^{\mathrm{c}}_{j,-}$). The continuity condition across e^{c}_j is then written
$$\int_{e^{\mathrm{c}}_j} j^h_{|F^{\mathrm{c}}_{j,+}} \cdot n_j = -\int_{e^{\mathrm{c}}_j} j^h_{|F^{\mathrm{c}}_{j,-}} \cdot n_j \quad \left(\stackrel{\mathrm{def}}{=} \mathbb{J}_j \right).$$

As a consequence, a discrete current is entirely determined by the fluxes $\mathbb{J}_j$ across the edges of the surface mesh $\mathscr{T}_{2h}(\Sigma)$. We associate with these degrees of freedom, a basis m_j of M^h, where j stands for the index of the edges e^{c}_j of $\mathscr{T}_{2h}(\Sigma)$.

Let us finally give some details about the computation of the matrices C^h_{c} and C^h_{f}. For the definition of $c^h_{\mathrm{c}}(.,.)$ and $c^h_{\mathrm{f}}(.,.)$, we use an approximation of $c_{\mathrm{c}}(.,.)$ and $c_{\mathrm{f}}(.,.)$ by using the quadrature formulas which are the equivalent of (53) for surface integrals. We then have:

$$\begin{aligned}
(C_{\mathrm{c}})_{j,i} &= \oint_{\Sigma} n \wedge (v^{\mathrm{c}}_i \wedge n) \cdot m_j = \sum_{F \in \mathscr{T}^{2h}(\Sigma)} \frac{\mathrm{meas}(F)}{4} \sum_{\ell=1}^{4} \left(v^{\mathrm{c}}_i \cdot m_j \right)_{|F}(S^F_\ell), \\
(C_{\mathrm{f}})_{j,k} &= \oint_{\Sigma} n \wedge (v^{\mathrm{f}}_k \wedge n) \cdot m_j = \sum_{F \in \mathscr{T}^{h}(\Sigma)} \frac{\mathrm{meas}(F)}{4} \sum_{\ell=1}^{4} \left(v^{\mathrm{f}}_k \cdot m_j \right)_{|F}(S^F_\ell),
\end{aligned} \tag{59}$$

where indexes i and j refer to the edges e^{c}_i and e^{c}_j of the coarse mesh ($e^{\mathrm{c}}_j \in \Sigma$), while index k is linked to the edges e^{f}_k of the fine grid.

To assemble in practice these matrices, it is useful to use the classical reference element method. In our case, the reference element is a square of side length $2h$. Using the numbering of the local 4 coarse edges and 12 fine edges indicated in Fig. 4, we get the following expressions for the 4×12 and 4×4 elementary matrices $(\hat{C}_{\mathrm{f}})$ and $(\hat{C}_{\mathrm{c}})$:

$$\hat{C}_{\mathrm{c}} = \frac{1}{4} \begin{bmatrix} 1 & 1 & 0 & 0 \\ -1 & -1 & 0 & 0 \\ 0 & 0 & -1 & -1 \\ 0 & 0 & 1 & 1 \end{bmatrix}, \tag{60}$$

$$\hat{C}^t_{\mathrm{f}} = \frac{1}{8} \begin{bmatrix} 1 & 3 & 2 & 6 & 1 & 3 & 0 & 0 & 0 & 0 & 0 & 0 \\ -3 & -1 & -6 & -2 & -3 & -1 & 0 & 0 & 0 & 0 & 0 & 0 \\ 0 & 0 & 0 & 0 & 0 & 0 & -3 & -1 & -6 & -2 & -3 & -1 \\ 0 & 0 & 0 & 0 & 0 & 0 & 1 & 3 & 2 & 6 & 1 & 3 \end{bmatrix}. \tag{61}$$

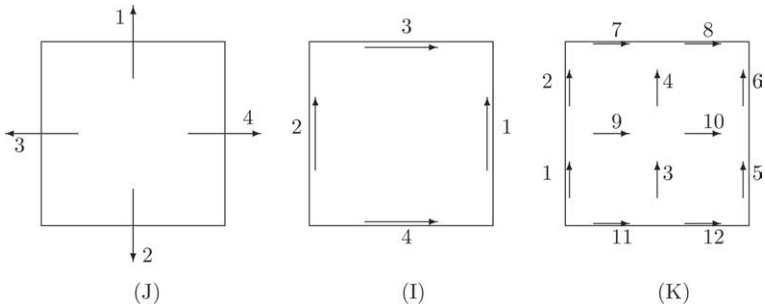

Fig. 4. Local numbering of the degrees of freedom: (*I*) (respectively, (*K*)) corresponds to the circulation on a coarse (respectively, fine) edge. (*J*) corresponds to the fluxes for the current.

The matrices C_c and C_f are then deduced from the elementary matrices $\hat{C}_c$ and $\hat{C}_f$ by standard techniques (we omit the details).

Remark 5. We have tested another choice for the approximation of the space M. It corresponds to using surface edge elements based on the coarse surface mesh. This space is deduced from the space M_h described above by applying to the vector fields a rotation of angle $\pi/2$ in the plane tangent to Σ. One can note that it also corresponds to the space of tangential traces of the discrete electric fields V_c^h, i.e., in the coarse grid domain. We obtain a non-conforming approximation since this space is no longer a subspace of the continuous space M: indeed, the tangential components are continuous across the edges of the surface mesh, but not the normal component. Our reason for testing this choice was linked to the fact that the structure of the resulting coupling matrix Q_h is simpler because it is sparser. Unfortunately, the numerical experiments we have performed seem to indicate that the resulting scheme, although stable, is not convergent! Such an observation, which still has to be understood from a theoretical point of view, seems to be in contradiction with the theoretical convergence results of [3] where non-conforming surfacic edge type elements are also considered for the approximation of J. However, in [3], the electric field is not approximated with the same edge elements space. Moreover, only the static problem is treated and the question of mesh refinement in time is not considered.

4.3. Existence of the discrete solution. Stability

4.3.1. Well-posedness

Thanks to (61), it is possible to check that the kernel of $(C_f^h)^*$ is $\{0\}$, hence to deduce that the scheme is well defined. The proof is as follows.

Let $\mathbb{J}$ be some vector in $\ker(C_f^h)^*$ and e_j^c be some coarse edge of $\mathscr{T}_{2h}(\Sigma)$. We denote by $F_{j,+}^c$ the adjacent face which is defined as in Section 4.2. We also denote $e_{j'}^c$ the edge of $F_{j,+}^c$ which is opposite to e_j^c. The line joining the middle of e_j^c and $e_{j'}^c$ is made of two fine edges, namely

$$e_k^f \quad \text{and} \quad e_{k'}^f.$$

This corresponds to the situation of Fig. 4.

From (61), it is easy to see that the equations $n^o k$ and $n^o k'$ of $(C_f^h)^* \mathbb{J} = 0$ give

$$\tfrac{6}{8}\mathbb{J}_j \pm \tfrac{2}{8}\mathbb{J}_{j'} = 0, \quad \pm\tfrac{2}{8}\mathbb{J}_{j'} + \tfrac{6}{8}\mathbb{J}_{j'} = 0,$$

from which we deduce that $\mathbb{J}_{j'} = \mathbb{J}_j = 0$. This concludes the proof since the edge e_j^c is arbitrary (see Fig. 5).

Remark 6. The result is no longer true when J is discretized with the fine mesh (more precisely, the trace of the fine mesh).

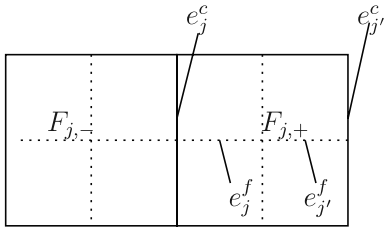

Fig. 5. The edges $e^c_j, e^c_{j'}$ and $e^f_k, e^f_{k'}$. The continuous (respectively, dotted) lines represent the trace of the coarse (respectively, fine) grid.

4.3.2. Stability condition

Another interesting point is to look at the CFL condition associated with the scheme. We return to the abstract CFL condition (50), obtained in the previous section

$$\Delta t < \max\left(\frac{1}{\beta_c}, \frac{2}{\beta_f}\right).$$

Using Property (55) and Definition (45), we have more explicitly

$$\beta_f^2 = c_0^2 \sup_{\tilde{E}\in V_f^h} \frac{\oint_{\Omega_f} |\mathrm{curl}\tilde{E}|^2}{\oint_{\Omega_f} |\tilde{E}|^2}, \quad \beta_c^2 = c_0^2 \sup_{\tilde{E}\in V_c^h} \frac{\oint_{\Omega_c} |\mathrm{curl}\tilde{E}|^2}{\oint_{\Omega_c} |\tilde{E}|^2},$$

where c_0 is $(\epsilon_0\mu_0)^{-1/2}$. We use the bound

$$\beta_f^2 \leqslant \tilde{\beta}_f^2 = c_0^2 \sup_{\tilde{E}\in V_f^h} \sup_{K\in\mathscr{T}_h} \frac{\oint_K |\mathrm{curl}\tilde{E}|^2}{\oint_K |\tilde{E}|^2}.$$

The mesh being uniform, $\tilde{\beta}_f$ can be found explicitly by a simple diagonalization of a quadratic form in R^{12} (taking into account the 12 edges of a single element)

$$\tilde{\beta}_f^2 = \frac{2}{h^2} c_0^2 \sup_{\mathbf{v}\in\mathbf{R}^{12}} \frac{\mathscr{Q}(\mathbf{v})}{\|\mathbf{v}\|^2},$$

where the quadratic form $\mathscr{Q}(\mathbf{v})$ is given by

$$\begin{aligned}\mathscr{Q}(\mathbf{v}) = {} & (v_{11} - v_9 - v_2 + v_1)^2 + (v_{12} - v_{10} - v_4 + v_3)^2 + (v_{12} - v_{11} - v_8 + v_6)^2 + (v_{10} - v_9 - v_7 + v_5)^2 \\ & + (v_8 - v_7 - v_4 + v_2)^2 + (v_6 - v_5 - v_3 + v_1)^2.\end{aligned}$$

The quadratic form $\mathscr{Q}(\mathbf{v})$ can be diagonalized: 0, 4, and 6 are its eigenvalues with respective multiplicities 7, 3, and 2. We infer that $\tilde{\beta}_f^2$ is $\frac{12c_0^2}{h^2}$. In the same way, it is found that β_c^2 is bounded by $\tilde{\beta}_c^2 = \frac{12c_0^2}{4h^2}$ (the factor 4 is due to the doubled size of the element). Thus, we get the following sufficient condition for stability,

$$\Delta t < \frac{h}{\sqrt{3}c_0}.$$

An important remark is that this CFL condition is exactly the same as the one which gives stability of the two FDTD schemes in an infinite grid, when no coupling occur. It is certainly a strong point of our method.

4.4. Considerations about the convergence analysis

Up to now, there have been very few complete results concerning the error analysis of the mesh refinement methods which we presented in the previous section. This is why we shall now give some insights about what such an analysis could be and indicate some directions of research (some of them being already under way). In fact, it is natural to distinguish two sources of errors:

- The space discretization and the change of space step between Ω_c and Ω_f.
- The time stepping and the change of time step between Ω_c and Ω_f.

To analyze the error due to the space discretization, it suffices to look at the semi-discrete problem (15)–(17). The most natural idea is to adapt to time evolution problems the analysis of the mortar element method that has already been carried out for corresponding static elliptic problems. There are at least two ways to consider this question:

- Use the mixed finite element technology as it has already been done, for instance in [4] for the Laplace equation. In this case, as mentioned in Section 3.1, the main difficulty lies in the proof of a uniform inf–sup condition.
- Consider the mortar element method as a non-conforming finite element method of Maxwell's equations via a formal elimination of the Lagrange multiplier and try to apply the second Strang's lemma.

This second point of view is the one that was adopted in the initial work on the analysis of the mortar method [3]. It was successfully applied for (the elliptic version of) Maxwell's equations in [3] when the second family of edge elements [21] is used for the approximation of the electric field and non-conforming surface edge elements are used for the discretization of the surface current. To our knowledge, the extension of such results for the finite elements we are considering in this paper (edge elements of the first family for the approximation of the electric field and conforming surfacic $H(\mathrm{div})$ elements for the surface current) remains an open problem.

The error due to the time discretization appears to be a more original issue. It has already been investigated in the case of the 1-D wave equation, [11,12]. Actually, if we apply our general method to the 1-D problem with the splitting $\Omega_f = \mathbf{R}^+$ and $\Omega_f = \mathbf{R}^-$: the spaces V_f and V_c are $H^1(\mathbf{R}^+)$ and $H^1(\mathbf{R}^-)$, W_f and W_c are $L^2(\mathbf{R}^+)$ and $L^2(\mathbf{R}^-)$, and the space M for the multiplier is simply reduced to $\mathbf{R}$. For the discretization, P^1 finite elements are used for the V-spaces and P^0 for the W-spaces (note that in the 1-D case, the question of the space approximation for the current does not pose any difficulty); using a mass lumping procedure, it is found that the scheme reduces to the 1-D FDTD scheme for the nodes not located at the interface; for the degrees of freedom located in the vicinity of the interface, an original coupling scheme is thus derived. It is possible to eliminate the current (a simple number) in these equations; we then obtain a finite difference scheme which coincides with the scheme derived in [11] and studied in [12]. We refer the reader to Collino et al. [12] for the results of the analysis of the scheme. This (non-standard) analysis essentially leads to an L^2 error estimate in $O(h^{3/2})$, assuming that the CFL number is kept constant: this loss of one half-power of h is a consequence of the off-centered nature or the time discretization of the transmission conditions. However, this $O(h^{3/2})$ error appears to be confined in the neighborhood of the interface and we conjecture that one recovers an $O(h^2)$ error estimate away from the interface.

5. Numerical aspects

We give in this section some hints about the implementation of our refinement method. We also present some numerical experiments.

5.1. Algorithm

5.1.1. Description of the algorithm

The time recursion can be solved along the following lines of:

- Apply scheme (24) on the time interval $[n\Delta t, 2n\Delta t]$, the source term $\mathbb{J}^{2n+1}$ being set to zero:

$$\begin{cases} \mathbb{H}_{\mathrm{f}}^{n+\frac{1}{2}} = \mathbb{H}_{\mathrm{f}}^{n-\frac{1}{2}} - \Delta t\left(M_H^{\mathrm{f}}\right)^{-1}(B_{\mathrm{f}})^*\mathbb{E}_{\mathrm{f}}^n, \\ \tilde{\mathbb{E}}_{\mathrm{f}}^{n+1} = \mathbb{E}_{\mathrm{f}}^n + \Delta t\left(M_E^{\mathrm{f}}\right)^{-1}B_{\mathrm{f}}\mathbb{H}_{\mathrm{f}}^{n+\frac{1}{2}}, \\ \begin{cases} \tilde{\mathbb{H}}_{\mathrm{f}}^{n+\frac{3}{2}} = \mathbb{H}_{\mathrm{f}}^{n+\frac{1}{2}} - \Delta t\left(M_H^{\mathrm{f}}\right)^{-1}(B_{\mathrm{f}})^*\tilde{\mathbb{E}}_{\mathrm{f}}^{n+1}, \\ \tilde{\mathbb{E}}_{\mathrm{f}}^{n+2} = \tilde{\mathbb{E}}_{\mathrm{f}}^{n+1} + \Delta t\left(M_E^{\mathrm{f}}\right)^{-1}B_{\mathrm{f}}\tilde{H}_{\mathrm{f}}^{n+\frac{3}{2}}, \end{cases} \end{cases} \quad \begin{cases} \mathbb{H}_{\mathrm{c}}^{n+1} = \mathbb{H}_{\mathrm{c}}^{n-1} - 2\Delta t\left(M_H^{\mathrm{c}}\right)^{-1}(B_{\mathrm{c}})^*\mathbb{E}_{\mathrm{c}}^n, \\ \tilde{\mathbb{E}}_{\mathrm{c}}^{n+2} = \mathbb{E}_{\mathrm{c}}^n + 2\Delta t\left(M_E^{\mathrm{c}}\right)^{-1}B_{\mathrm{c}}H_{\mathrm{c}}^{n+1}. \end{cases}$$

- Solve the linear system (the matrix Q is given in (32))

$$Q\mathbb{J}^{n+1} = C_{\mathrm{f}}\frac{\tilde{\mathbb{E}}_{\mathrm{f}}^{n+2} + 2\tilde{\mathbb{E}}_{\mathrm{f}}^{n+1} + \mathbb{E}_{\mathrm{f}}^n}{4} - C_{\mathrm{c}}\frac{\tilde{\mathbb{E}}_{\mathrm{c}}^{n+2} + \mathbb{E}_{\mathrm{c}}^n}{2},$$

- Correct the previous time step:

$$\begin{cases} \mathbb{E}_{\mathrm{c}}^{n+2} = \tilde{\mathbb{E}}_{\mathrm{c}}^{n+2} - 2\Delta t\left(M_E^{\mathrm{c}}\right)^{-1}(C_{\mathrm{c}})^*\mathbb{J}^{n+1}, \\ \mathbb{E}_{\mathrm{f}}^{n+1} = \tilde{\mathbb{E}}_{\mathrm{f}}^{n+1} + \Delta t\left(M_E^{\mathrm{f}}\right)^{-1}(C_{\mathrm{f}})^*\mathbb{J}^{n+1}, \\ \mathbb{H}_{\mathrm{f}}^{n+\frac{3}{2}} = \mathbb{H}_{\mathrm{f}}^{n+\frac{1}{2}} - \Delta t\left(M_H^{\mathrm{f}}\right)^{-1}(B_{\mathrm{f}})^*\mathbb{E}_{\mathrm{f}}^{n+1}, \\ \mathbb{E}_{\mathrm{f}}^{n+2} = \mathbb{E}_{\mathrm{f}}^{n+1} + \Delta t\left(M_E^{\mathrm{f}}\right)^{-1}B_{\mathrm{f}}H_{\mathrm{f}}^{n+\frac{3}{2}} + \Delta t\left(M_E^{\mathrm{f}}\right)^{-1}(C_{\mathrm{f}})^*\mathbb{J}^{n+1}. \end{cases}$$

With respect to the simple marching of the Yee scheme in each grid, the main new step introduced by the mesh refinement procedure is the solution of the linear system.

The matrix Q can be constructed by assembling all the matrices C_{c}, C_{f}, M_E^{c}, M_E^{f}, B_{f}, and M_H^{f}, and computing the different products appearing in formula (32). To obtain a simpler implementation, it is worthwhile to notice that computing a column of the matrix Q simply amounts to applying the explicit Yee scheme in each grid during one coarse time step $2\Delta t$ for a given current. More precisely, let $\mathbb{J}$ be some current, the computation of $Q\mathbb{J}$ can be obtained through the following procedure:

- Set the initial conditions $\mathbb{E}_{\mathrm{f}}^0 = \mathbb{H}_{\mathrm{f}}^{-1/2} = \mathbb{E}_{\mathrm{c}}^0 = \mathbb{H}_{\mathrm{c}}^{-1} = 0$.
- Apply scheme (24) on the time interval $[0, 2\Delta t]$, the source term $\mathbb{J}$ being given:

$$\begin{cases} \mathbb{H}_{\mathrm{f}}^{1/2} = \mathbb{H}_{\mathrm{f}}^{-1/2} - \Delta t\left(M_H^{\mathrm{f}}\right)^{-1}(B_{\mathrm{f}})^*\mathbb{E}_{\mathrm{f}}^0, \\ \mathbb{E}_{\mathrm{f}}^1 = \mathbb{E}_{\mathrm{f}}^0 + \Delta t\left(M_E^{\mathrm{f}}\right)^{-1}\left(B_{\mathrm{f}}\mathbb{H}_{\mathrm{f}}^{1/2} + C_{\mathrm{f}}^*\mathbb{J}\right), \\ \begin{cases} \mathbb{H}_{\mathrm{f}}^{3/2} = \mathbb{H}_{\mathrm{f}}^{1/2} - \Delta t\left(M_H^{\mathrm{f}}\right)^{-1}(B_{\mathrm{f}})^*\mathbb{E}_{\mathrm{f}}^1, \\ \mathbb{E}_{\mathrm{f}}^2 = \mathbb{E}_{\mathrm{f}}^1 + \Delta t\left(M_E^{\mathrm{f}}\right)^{-1}\left(B_{\mathrm{f}}H_{\mathrm{f}}^{3/2} + C_{\mathrm{f}}^*\mathbb{J}\right), \end{cases} \end{cases} \quad \begin{cases} \mathbb{H}_{\mathrm{c}}^1 = \mathbb{H}_{\mathrm{c}}^{-1} - \Delta t\left(M_H^{\mathrm{c}}\right)^{-1}(B_{\mathrm{c}})^*\mathbb{E}_{\mathrm{c}}^0, \\ \mathbb{E}_{\mathrm{c}}^2 = \mathbb{E}_{\mathrm{c}}^0 + \Delta t\left(M_E^{\mathrm{c}}\right)^{-1}\left(B_{\mathrm{c}}H_{\mathrm{c}}^1 - C_{\mathrm{c}}^*\mathbb{J}\right). \end{cases}$$

- Compute

$$Q\mathbb{J} = C_{\mathrm{c}}\frac{\mathbb{E}_{\mathrm{c}}^2 + \mathbb{E}_{\mathrm{c}}^0}{2} - C_{\mathrm{f}}\frac{\mathbb{E}_{\mathrm{f}}^2 + 2\mathbb{E}_{\mathrm{f}}^1 - \mathbb{E}_{\mathrm{f}}^0}{4}.$$

In practice, the above procedure is applied for each basis function of the space M^h. The scheme being explicit, it is possible to restrict the integration of the Yee scheme to small boxes of some few meshes around the coarse edge associated with the considered basis function. Matrix Q has a lot of good properties: it is real, symmetric, sparse (it can be verified that Q possesses at most 25 non-zero elements per line), and well-conditioned (the conditioning number is found approximatively independent of the size of the fine box and ranges from 20 to 30 depending on the Courant number $\frac{c_0\Delta t}{h}$). The solution of the linear system can be found by a simple conjugate gradient algorithm. As an example, we take Ω_f to be a cubic domain $10h \times 12h \times 8h$. In this case, the size of the matrix is 1184 and the number of non-zero elements is 30,104, so that only 15,644 elements are stored since the matrix is symmetric. The skeleton of the matrix Q is shown in Fig. 6. We found numerically that only 37 iterations were required to achieve a relative error of 10^{-14} when $\frac{c_0\Delta t}{h} \simeq \frac{1}{\sqrt{3}}$.

5.1.2. A remark about how to take into account a conductor across an interface

It is of course possible (and essential for practical applications) to extend the method presented in this paper to the cases where perfectly conducting obstacles are located in the computational domain and cross the interface between the two grids. From the theoretical point of view, the only modification lies in the introduction of some new functional spaces M with a more involved definition. From a practical point of view, the change in the discrete space M^h is not very complicated, at least if it is assumed that the surface Γ of the conducting body can be approximated by a surface Γ_h which is a union of faces of the coarse and fine meshes with the additional geometrical property:

- If a portion Γ_h^{int} (of non-zero measure) of the surface Γ_h coincides with a part of the interface Σ, then Γ_h^{int} is made of a finite union of faces of the boundary mesh of Σ, i.e., of faces of the coarse grid mesh.
- If Γ_h crosses the interface Σ along a line, then this line is composed of segments of the coarse mesh.

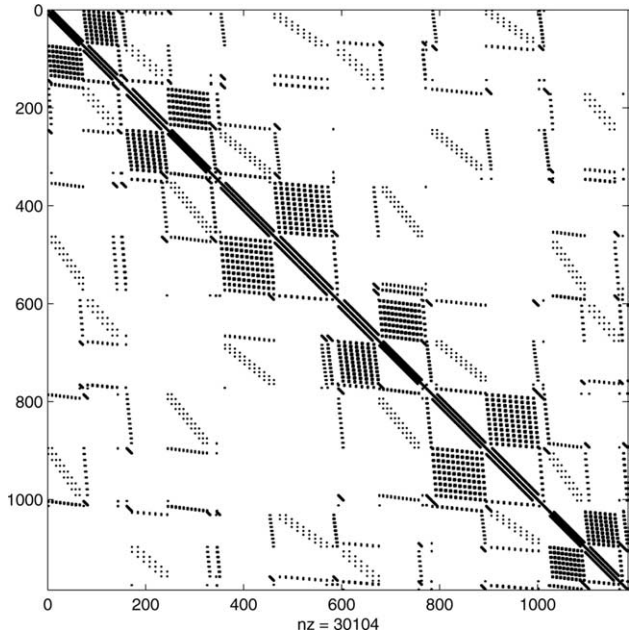

Fig. 6. Sparsity pattern of the matrix Q for a refined box Ω_f of size $10h \times 12h \times 8h$.

Note that these hypothesis imply in particular that when the fine box boundary crosses the conducting surface, it does so necessarily along squares of the coarse mesh or segments of the coarse mesh.

For each edge of $\mathscr{T}_{2h}(\Sigma)$, the number of degrees of freedom for the current J_h depends on the particular status of this edge:

- It may be 0: this case occurs when the edge is completely embedded inside Γ_h.
- It may be 1 in two situations:
  - The edge intersects Γ_h^{int} on one point or does not intersect Γ_h^{int}. Then, the support of the associated basis function is composed of the two squares on which lies the edge (exactly as in the case without conductor).
  - The edge intersects Γ_h^{int} along a segment and one of the two elements associated with the edge is embedded into Γ_h^{int}. In this case, the edge lies on the boundary of Γ_h^{int} and the support of the associated basis function is a single element.
- It may be 2. When a part of Γ_h crosses transversally the box, it draws a line on Σ. Any edge belonging to this line must support two degrees of freedom (because of the jump of the magnetic field across this line).

All that is described in more details in [14] where a simple algorithm for dealing with all the situations is also given.

5.2. Numerical results

The results that we present in this section correspond to scattering experiments of an incident plane wave whose propagation direction is parallel to one of the direction of the computational mesh, let us say $E^{\text{inc}}(x,y,z,t) = W(t - z/c_0)\hat{y}$. The computation of the complete solution is obtained with the so-called Huygens surface method: we define a cubic boundary as the Huygens surface and compute the total field inside this surface and the scattered field outside; technically, it amounts to correcting the formulae of the scheme that mix edges of different nature by the known incident field (see [15] for more details). On the outer boundary, we use a Perfectly Matched Layer with an artificial layer of width four coarse steps. The incident wave is approximated by an exact solution of the scheme in the coarse grid (practically, it is computed through the solution of a 1-D Yee scheme); by doing so, we guarantee that the numerical solution of the 3-D scheme in the free space is exactly the incident wave for the edges lying inside the Huygens surface and vanishes for the edges lying outside this surface.

In all experiments, the Huygens surface always surrounds the fine grid. The domain of computation is a cubic box of size 10 m. The wavelet is a Gaussian: $F(t) = 1000\exp(-(\frac{t-5t_0}{t_0})^2)$ and $t_0 = 10$ ns. The mesh in the coarse grid consists of cubes of size $2h = 0.25$. This corresponds roughly to 15 points per wavelength (measured with respect to the cutoff frequency of our incident signal). The ratio $\frac{c_0\Delta t}{h}$ is kept constant and equal to $0.95\frac{\sqrt{3}}{3}$.

Three experiments will be presented:

- An artificial diffraction by a local refinement of the mesh in the whole space: Section 5.2.1.
- The diffraction by a beveled wedge (a geometry that does not fit the mesh): Section 5.2.2.
- The diffraction by a resonant cavity with a small aperture: Section 5.2.3.

In the last two cases, a reference solution is computed with a very fine uniform grid of step size $\frac{2h}{4}$ and three computations are compared; the first one with a coarse grid ($2h$ everywhere), the second one with a fine grid everywhere (h everywhere) and finally, one with a coarse grid locally refined.

5.2.1. An academic example: refining a box in the whole space

We measure the effect of a simple grid refinement on the propagation of the incident plane wave in the free space. We repeat the same experiment for different grids, one with a coarse mesh without refinement, one with a fine mesh everywhere, and another one with a local refinement in a small parallelepipedic box of size $5h$, $6h$ and $4h$ in the respective directions x, y and z. A simulation with a very fine mesh is our reference solution. We examine the field at a coarse point located one coarse mesh behind the refined box. The comparison is shown in Fig. 7. We can see that all the curves look the same. Considering the error, we observe that the error with the refinement in the small box looks the same as that without any refinement. It means that for this degree of discretization, (about 15 points per wavelength), the error due to the local refinement can be neglected in view of the much larger classical errors due to dispersion. Some other experiments [14] show that the difference between fields computed in meshes with a refined box of size d and the field computed in a single coarse grid increases continuously with the size d of the refined box. This can be easily explained by the fact that the dispersion is lowest during the propagation of the wave inside the fine grid and so the larger the fine grid the larger the difference. To observe the error only due to the box, we have measured the ratio of the electric energy due to the component E_x and E_z (which ought to be very small) to the electric energy due to the component E_y; the result is that this ratio does not surpass 48 dB no matter what size of the box.

5.2.2. Scattering by a beveled wedge

We consider in this paragraph a case where the refinement is useful for diminishing numerical diffraction effects. We take a perfect conducting object with a geometry that does not fit the mesh; this requires the use of a staircase approximation of the geometry, clearly a difficult situation, especially when the scatterer has angular points. We create a fine grid around a beveled wedge as shown in Fig. 8. The results, depicted in Fig. 10, show that the error decreases with the local refinement and can even be as good as if the mesh were refined everywhere (Fig. 11). This might be explained by the fact that the error is mainly due to the singularity of the solution at the angle of the wedge, the error related to the dispersion effect being small (see Fig. 9).

5.2.3. The case of a Helmholtz resonator

We consider the scattering of a wave on a metallic cavity, the surface of a parallelepiped $\mathscr{C} = [0, 20h] \times [0, 20h] \times [0, 10h]$ minus a square (a window $\mathscr{W}$) slightly shifted with respect to the center

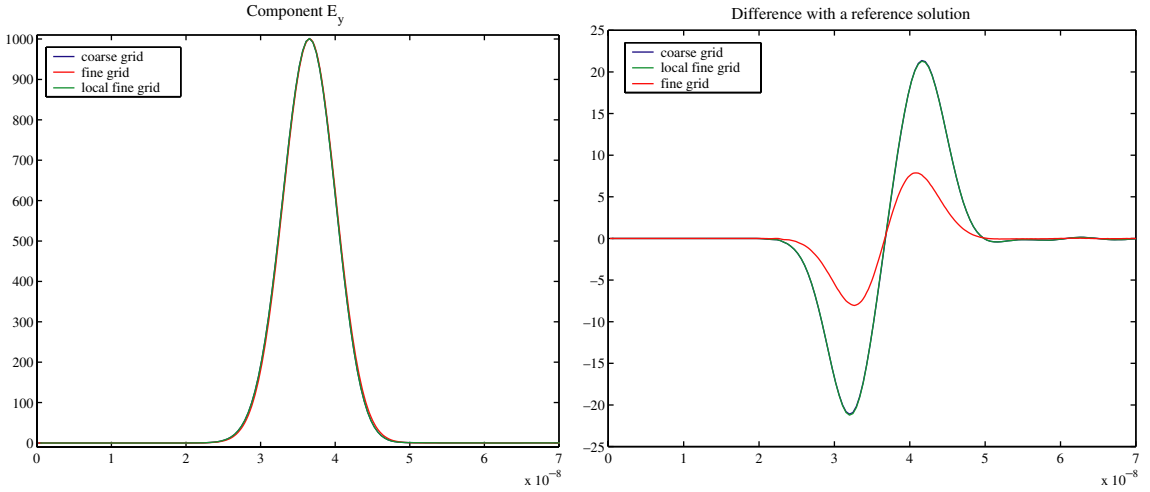

Fig. 7. Propagation in the free space: on the left, the field E_y versus time at a point located in the coarse mesh one step behind the refined cubic domain; on the right, the difference with a reference solution.

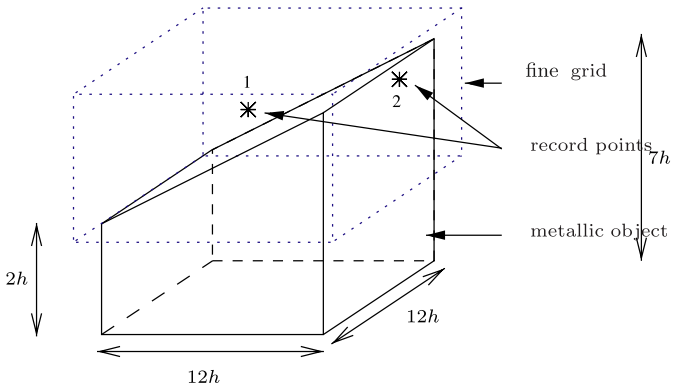

Fig. 8. Position of the fine grid with respect to the wedge.

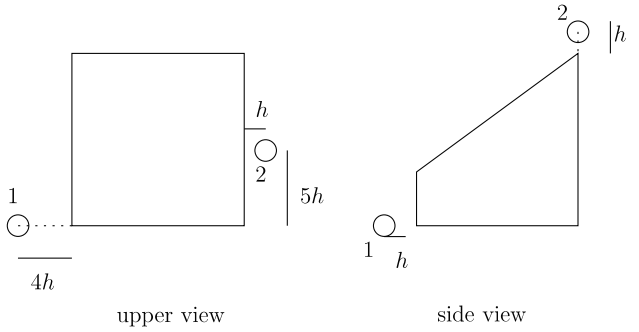

Fig. 9. Position of the fine grid with respect to the wedge.

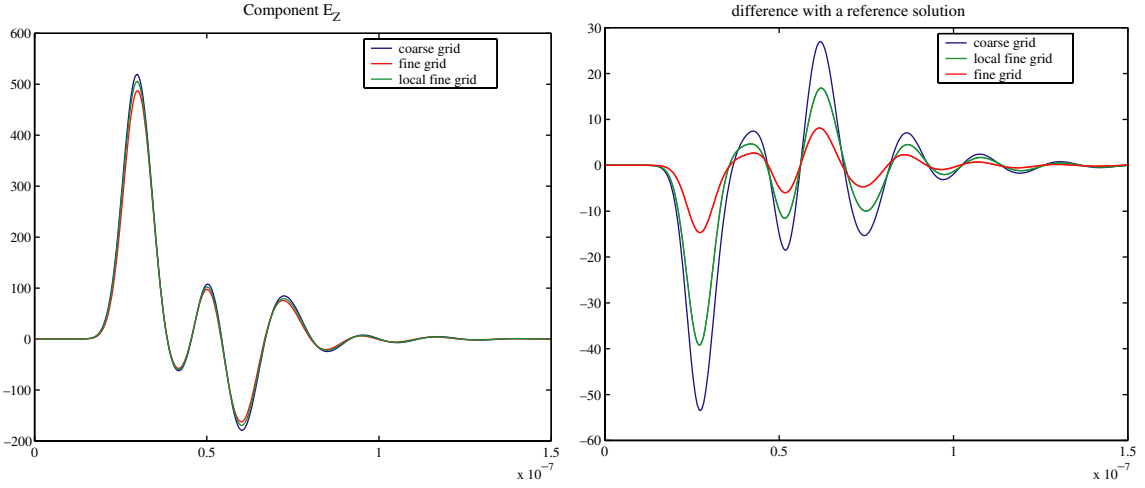

Fig. 10. The beveled wedge: E_z versus time at recording point 1.

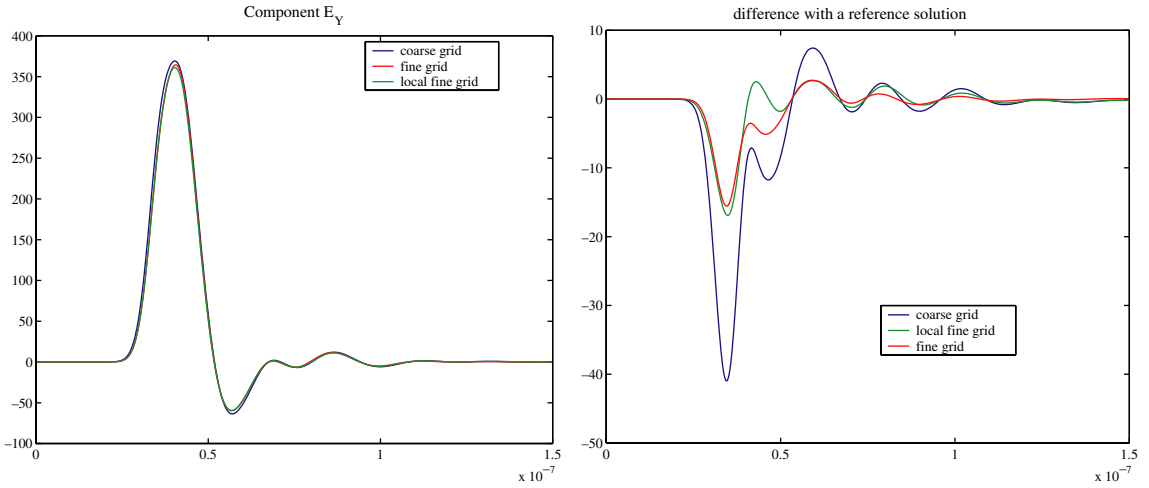

Fig. 11. The beveled wedge: E_y versus time at recording point 2.

of one of its faces: $\mathscr{W} = [7h, 11h] \times [7h, 11h] \times \{0\}$. We put a fine grid around the window ($\Omega_f = [6h,12h] \times [6h,12h] \times [-h,h]$) and record the field $\vec{E}$ at a point R located just inside the window and inside the coarse grid $R = (8h,8h,2h)$.

We illustrate the experiment in Fig. 12 and the corresponding results are presented in Fig. 13. The experiment with the local refinement gives results of the same quality as that with a fine grid throughout the domain. At the same time, the CPU time is increased by a factor 1.4 with the local refinement and by a factor 16 with the refinement in the whole domain.

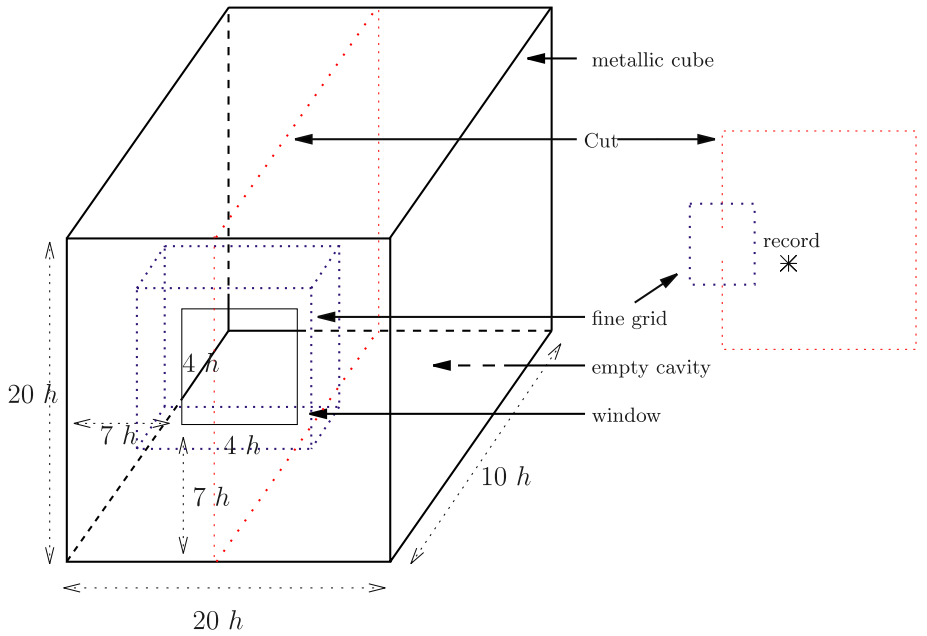

Fig. 12. An empty metallic cube has a window where the wave can enter and we record the solution inside the cube.

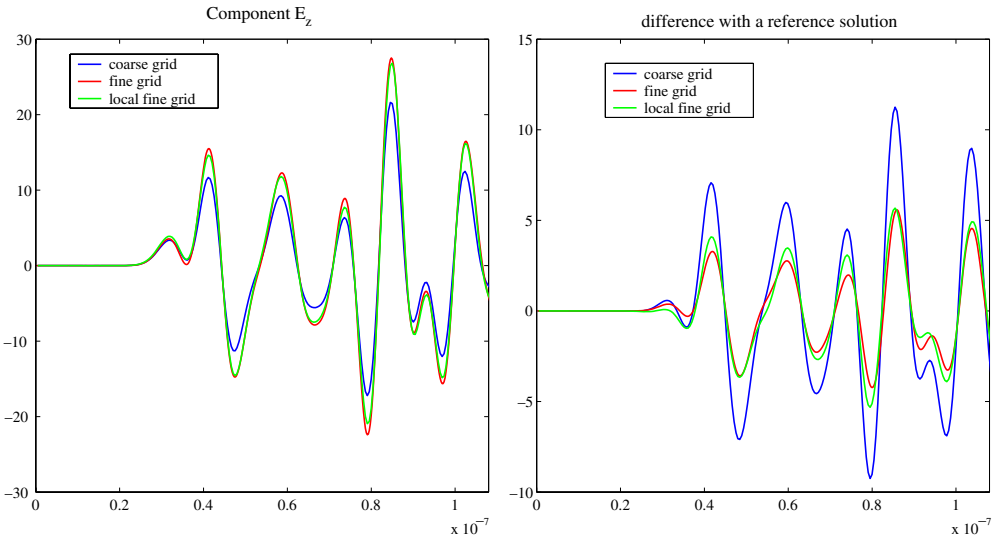

Fig. 13. Components E_z of the solution and the difference with a reference solution at the record point.

6. Conclusion

We have presented a contribution to space-time refinement methods for the numerical solution of time dependent Maxwell's equations. The new method we have proposed presents two main theoretical advantages over most of the solutions previously proposed in the literature:

- The first one is robustness. By construction, our method is conservative, which guarantees theoretically the stability. Other methods, such as interpolation methods, are quite difficult to analyze and may encounter some stability problems, [14]. Moreover, the stability condition is not affected by the mesh refinement procedure.
- The second one is its very general nature (see [16]). Although we have chosen to present, for the sake of simplicity, the method for mesh refinement for the Yee's scheme, our algorithm can be applied to a large class of methods allowing for the possibility of using different discretization inside each domain including various finite element methods on unstructured grids or finite element methods of different orders. Our procedure can also be applied to various physical problems such as elastic wave propagation [2] or fluid–structure interaction problems.

Regarding accuracy, a question which we have not treated in this paper from the theoretical point of view, some partial results are available in the literature in the 1-D case [12,17] where it is shown that our method has second order accuracy ($O(h^2)$ L^2-error estimates) in regions that avoid the interface (global L^2 error estimates only provide a $O(h^{3/2})$ accuracy, which is sharp). These results confirm the soundness of our approach and show a certain superiority of our method with respect to standard interpolation methods (which are generically first order accurate).

With respect to the usual explicit finite difference scheme, the additional cost of the method consists in assembling the matrix Q which permits us to calculate the electric current on the interface and inverting this matrix (which is sparse positive definite, and thus easily invertible by Cholesky or Conjugate Gradient) at each time step. We have shown an implementation of the computation of the matrix Q that aims at simplicity by exploiting the explicit nature of the interior scheme and which is very useful in practice.

Finally, our various 3-D numerical experiments illustrate the practical interest (in terms of a gain in computational time and memory storage) of using a space-time mesh refinement procedure for diffraction problems. Let us mention that, even though the results we have presented have been obtained with a single 1–2 mesh refinement, the use of successive mesh refinements can obviously be used and can be implemented in a recursive way.

To conclude, we mention that, apart from the extension of our method to other physical problems, our research is continuing in several directions:

- The extension to more general refinements (typically $(\Delta t/p, \Delta t/q)$ where (p,q) are integers).
- The improvement of the accuracy of the method (including in the neighborhood of the interface).
- The coupling of this method with the fictitious domain method introduced in [13], whose philosophy is close to the one of the conservative mesh refinement method.

References

[1] A. Bamberger, R. Glowinski, Q.H. Tran, A domain decomposition method for the acoustic wave equation with discontinuous coefficients and grid change, SIAM J. Numer. Anal. 34 (2) (1997) 603–639.
[2] E. Bécache, P. Joly, J. Rodríguez, Space-time mesh refinement for elastodynamics. Numerical results, Comput. Meth. Appl. Mech. Eng. 194 (2-5) (2005) 355–366.
[3] F.B. Belgacem, A. Buffa, Y. Maday, The mortar finite element method for 3d Maxwell equations: first results, SIAM J. Numer. Anal. 39 (3) (2001) 880–901.
[4] F.B. Belgacem, The mortar finite element method with Lagrange multipliers, Numer. Math. 84 (1999) 173–197.
[5] F. Brezzi, M. Fortin, Mixed and Hybrid Finite Element MethodsSpringer series in computational mathematics, vol. 15, Springer, Berlin, 1991.
[6] A. Buffa, P. Ciarlet Jr., On traces for functional spaces related to Maxwell's equations. ii. Hodge decompositions on the boundary of Lipschitz polyhedra and applications, Math. Meth. Appl. Sci. 24 (1) (2001) 31–48.
[7] M.W. Chevalier, R.J. Luebbers, FDTD local grid with material traverse, IEEE Trans. Antenn. Propagat. 45 (3) (1997) 411–421.
[8] G. Cohen, Higher-order Numerical Methods for Transient Wave Equations. Scientific Computation, Springer, Berlin, New York, 2002.
[9] F. Collino, T. Fouquet, P. Joly. Analyse numérique d'une méthode de raffinement de maillage espace-temps pour l'équation des ondes, Technical Report 3474, INRIA, Aout, 1998.
[10] F. Collino, T. Fouquet, P. Joly, Une méthode de raffinement de maillage espace-temps pour le système de maxwell en dimension un, CR Acad. Sci. Paris 328 (1999) 263–268.
[11] F. Collino, T. Fouquet, P. Joly, A conservative space-time mesh refinement method for the 1-d wave equation. Part I: Construction, Numerische mathematik 95 (2003) 197–221.
[12] F. Collino, T. Fouquet, P. Joly, A conservative space-time mesh refinement method for the 1-d wave equation. Part II: Analysis, Numerische mathematik 95 (2003) 223–251.
[13] F. Collino, P. Joly, F. Millot, Fictitious domain method for unsteady problems: application to electromagnetic scattering, J. Comput. Phys. 138 (1997) 907–938.
[14] T. Fouquet, Raffinement de maillage spatio temporel pour les équations de Maxwell, Ph.D. Thesis, Université Paris IX Dauphine, June, 2000.
[15] S.D. Gedney, F. Lansing, Computational electrodynamics the finite-difference time-domain method, in: A. Taflove (Ed.), Chapter Explicit Time-domain Solution of Maxwell's Equations Using Nonorthogonal and Unstructured Grids, Artech House, Boston, London, 1995, pp. 343–393.
[16] P. Joly, Variational methods for time-dependent wave propagation problems, in: Computational Wave Propagation. Direct and Inverse Problems, Springer, Berlin, 2003, pp. 201–264.
[17] P. Joly, J. Rodríguez, An error analysis of conservative space-time mesh refinement methods for the 1-d wave equation (submitted).
[18] I.S. Kim, W.J.R. Hoefer, A local mesh refinement algorithm for the time-domain finite-difference method to solve Maxwell's equations, IEEE Trans. Microwave Theory Tech. 38 (6) (1990) 812–815.
[19] K.S. Kunz, L. Simpson, A technique for increasing the resolution of finite-difference solutions to the Maxwell equations, IEEE Trans. Electromagn. Compat. EMC-23 (1981) 419–422.

[20] P. Monk, Sub-gridding FDTD schemes, ACES J. 11 (1996) 37–46.
[21] J. Nedelec, A new family of mixed finite elements in $\mathbb{R}^3$, Numer. Math. 50 (1986) 57–81.
[22] D.T. Prescott, N.V. Shuley, A method for incorporating different sized cells into the finite-difference time-domain analysis technique, IEEE Microwave Guided Wave Lett. 2 (1992) 434–436.
[23] K. Yee, Numerical solution of initial boundary value problems involving Maxwell's equations in isotropic media, IEEE Trans. Antenn. Propagat. (1966) 302–307.